

1 **Inter-tissue convergence of gene expression during ageing suggests age-** 2 **related loss of tissue and cellular identity**

3

4 Hamit Izgi¹, DingDing Han^{2,*}, Ulas Isildak¹, Shuyun Huang², Ece Kocabiyik¹, Philipp Khaitovich^{3*},
5 Mehmet Somel^{1*}, Handan Melike Dönertaş^{4,5*}

6

7 ¹ Department of Biological Sciences, Middle East Technical University, Ankara, Turkey

8 ² CAS Key Laboratory of Computational Biology, CAS-MPG Partner Institute for Computational Biology, Shanghai Institutes for
9 Biological Sciences, Chinese Academy of Sciences, Shanghai, China

10 ³ Center for Neurobiology and Brain Restoration, Skolkovo Institute of Science and Technology, Moscow, Russia

11 ⁴ European Molecular Biology Laboratory, European Bioinformatics Institute EMBL-EBI, Wellcome Trust Genome Campus,
12 Cambridge, UK

13 ⁵ Leibniz Institute on Aging - Fritz Lipmann Institute (FLI), Beutenbergstraße 11, 07745, Jena, Germany

14 * present address: Department of Clinical Laboratory, Shanghai Children's Hospital, Shanghai Jiaotong University, Shanghai,
15 China

16 *Correspondence: melike.donertas@leibniz-flj.de (H.M.D), msomel@metu.edu.tr (M.S.), P.Khaitovich@skoltech.ru (P.K)

17

18 **Abstract (124/150 words)**

19 Developmental trajectories of gene expression may reverse in their direction during ageing, a
20 phenomenon previously linked to cellular identity loss. Our analysis of cerebral cortex, lung, liver and
21 muscle transcriptomes of 16 mice, covering development and ageing intervals, revealed widespread
22 but tissue-specific ageing-associated expression reversals. Cumulatively, these reversals create a
23 unique phenomenon: mammalian tissue transcriptomes diverge from each other during postnatal
24 development, but during ageing, they tend to converge towards similar expression levels, a process we
25 term Divergence followed by Convergence, or DiCo. We found that DiCo was most prevalent among
26 tissue-specific genes and associated with loss of tissue identity, which is confirmed using data from
27 independent mouse and human datasets. Further, using publicly available single-cell transcriptome
28 data, we showed that DiCo could be driven both by alterations in tissue cell type composition and also
29 by cell-autonomous expression changes within particular cell types.

30

31 **Keywords**

32 Ageing, development, transcriptome, mouse, reversal

33 Introduction

34 Development and ageing in multicellular organisms are highly intertwined processes. On the one hand,
35 certain ageing-related phenotypes, such as presbyopia and osteoporosis (Luegmayr et al. 2004) are
36 believed to represent the continuation of developmental processes into adulthood (Blagosklonny 2006;
37 de Magalhães and Church 2005)). Such cases of “runaway development” or higher than optimal
38 function during ageing (recognized as the hyperfunction theory of ageing (Gems and Partridge 2013)),
39 may arise due to declined natural selection pressure failing to optimise expression regulation after
40 sexual reproduction starts (Fisher, 1930; Medawar, 1953; Williams, 1957). Indeed, recent experimental
41 studies in *C. elegans* show that senescence phenotypes promoted by insulin-IGF-1 signalling pathways
42 support the hyperfunction theory (Lind et al. 2019; Ezcurra et al. 2018)). On the other hand, molecular
43 studies have also reported a reversal of the ageing transcriptome towards pre-adult levels in various
44 contexts, including primate brain regions (Somel et al. 2010; Dönertaş et al. 2017; Colantuoni et al.
45 2011), and mouse liver and kidney (Anisimova et al. 2020). Studying the functional consequences of
46 this reversal pattern in the ageing human brain, we previously interpreted it as an indication of loss of
47 cellular identity in neurons, possibly exacerbated by a reduction in the relative frequencies of neurons
48 (Dönertaş et al. 2017). Such changes, in turn, could be caused by the accumulation of stochastic
49 damage at the genetic, epigenetic, and proteomic levels over an adult lifetime, causing deregulation of
50 gene expression networks.

51

52 Several major questions remain. First, the prevalence of reversal phenotypes across tissues is unclear,
53 as most research has been conducted in the brain (Somel et al. 2010; Dönertaş et al. 2017). A second
54 question pertains to the similarity of reversal-exhibiting genes and pathways across tissues. Ageing-
55 related expression changes are partly shared among organs (Zahn et al. 2007), and reversal trends are
56 also shared across different regions of the primate brain (Dönertaş et al. 2017). Distinct tissues might
57 hence show parallel reversal patterns. Alternatively, as mammalian tissues diverge from each other
58 during development in their transcriptome profiles (Cardoso-Moreira et al. 2019), one may hypothesise
59 that during ageing, tissues converge back toward similar transcriptome profiles. Such a putative late-
60 age convergence phenomenon would be consistent with the notion of ageing-related cellular identity
61 loss (Yang et al. 2019; Dönertaş et al. 2017). A final question concerns the mechanism behind the
62 observed reversal trends at the bulk tissue level. Specifically, the contribution of cell type composition

63 and cell-autonomous changes to the reversals at the tissue level remains unexplored.

64

65 Documenting the reversal phenomenon is critical to better understand the proximate mechanisms of
66 mammalian ageing, and its ultimate mechanisms, such as the stochastic disruption versus continued
67 expression of developmental genes. However, such work has been limited by the scarcity of studies
68 that include both development and ageing periods of the same organism and across different tissues.
69 This work presents an age-series analysis of bulk transcriptome profiles of mice, including samples of
70 four tissues across postnatal development and ageing periods covering the whole postnatal lifespan.
71 Using this dataset, we study the prevalence, mechanisms, and functional consequences of the reversal
72 phenomenon in different mouse tissues. We further test the related hypothesis of tissue convergence
73 during ageing and investigate the contribution of cell type composition and cell-autonomous changes.

74

75 **Results**

76 We generated bulk RNA-seq data from 63 samples covering the cerebral cortex (which we refer to as
77 cortex), liver, lung, and skeletal muscle (which we refer to as muscle) of 16 male C57BL/6J mice, aged
78 between 2 to 904 days of postnatal age (Methods). As mice reach sexual maturity by around two months
79 (Tacutu et al. 2018), we treated samples from individuals aged between 2 and 61 days (n=7) as the
80 development series, and those aged between 93 and 904 days (which roughly correspond to 80-year-
81 old humans (Flurkey, M. Curren, and Harrison 2007)) (n=9) as the ageing series (**Figure 1-figure**
82 **supplement 1**). The final dataset contained n=15,063 protein-coding genes expressed in at least 25%
83 of the 63 samples (one 904 days old mouse lacked cortex data).

84

85

86

87

88

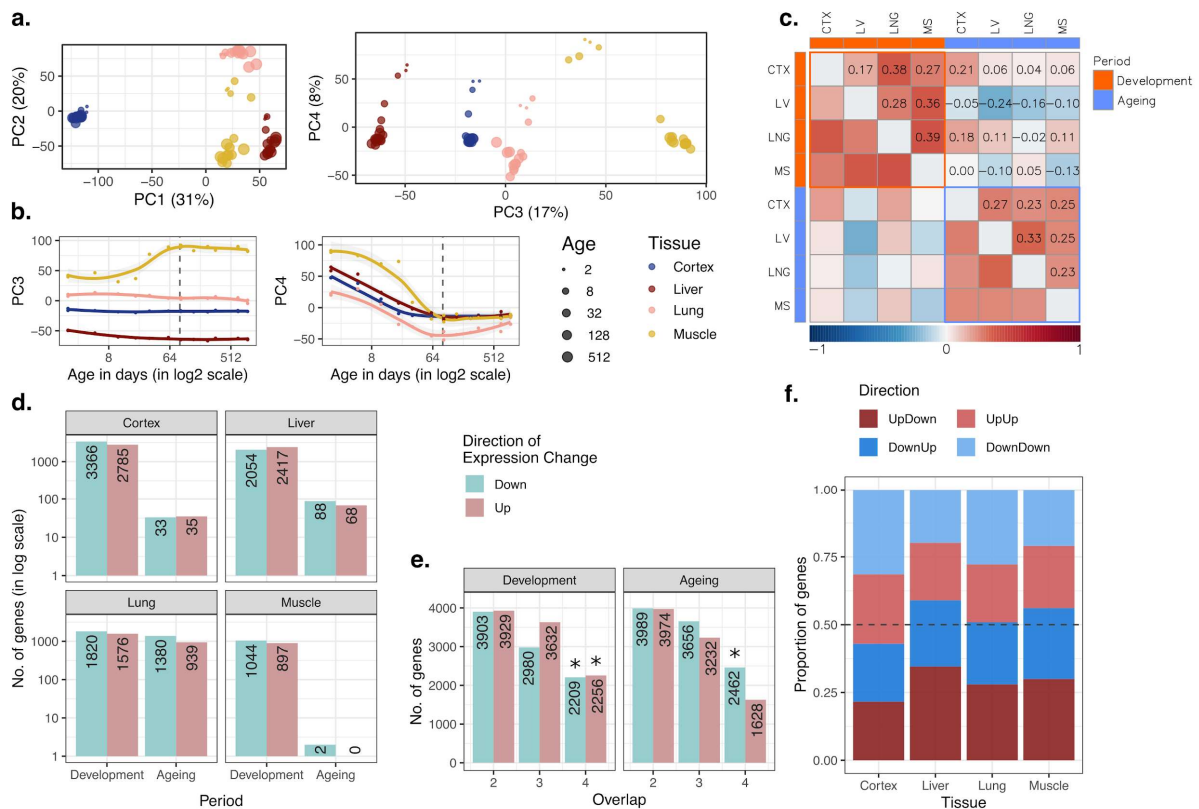
89

90

91

92

93 **Figure 1. Data summary and age-related expression patterns**



94

95 **a)** Principal components analysis (PCA) of expression levels of 15,063 protein-coding genes across four tissues of

96 16 mice. Values in parentheses show the variation explained by each component. **b)** Age trajectories of PC3 (left)

97 and PC4 (right). Spearman's correlation coefficients between PC4 and age in each tissue in development range

98 between 0.88 and 0.99 (See **Figure 1-source data** for all tests). The dashed vertical line indicates 90 days of age,

99 separating development and ageing periods. Age distribution of samples are given in **Figure 1-figure supplement**

100 **1. c)** Similarity between the age-related gene expression changes (Spearman's correlation coefficient between

101 expression and age without a significance cutoff) across tissues in development and ageing. Similarities were

102 calculated using Spearman's correlation coefficient between expression-age correlations across tissues. CTX:

103 cortex, LV: liver, LNG: lung, MS: muscle. **d)** The number of significant age-related genes in each tissue (FDR

104 corrected p -value < 0.1). **e)** Shared age-related genes among tissues identified without using a significance cutoff.

105 The x-axis shows the number of tissues among which age-related genes are shared. Significant overlaps are

106 indicated with an asterisk (*) (**Figure 1-figure supplement 4**). **f)** The proportion of age-related expression change

107 trends (no significance cutoff was used) in each tissue across the lifetime. UpDown: up-regulation in development

108 and down-regulation in the ageing; DownUp: down-regulation in development and up-regulation in the ageing;

109 UpUp: up-regulation in development and up-regulation in the ageing; DownDown: down-regulation in development

110 and down-regulation in ageing. We confirmed the robustness of the results using VST normalisation in **Figure 1-**

111 **figure supplement 10.**

112 **Tissues diverge during postnatal development.** Consistent with earlier work (Brawand et al. 2011;
113 Cardoso-Moreira et al. 2019), we found that variation in gene expression is largely explained by tissue
114 differences, such that the first three principal components (PCs) separate samples according to tissue
115 (ANOVA $p < 10^{-20}$ for PC1-3, **Figure 1-source data**), with the cortex most distant from the others (**Figure**
116 **1a**). Meanwhile, PC4, which explains 8% of the total variance, displayed a shared age-effect across
117 tissues in development (Spearman's correlation coefficient $\rho = [-0.88, -0.99]$, nominal $p < 0.01$ for each
118 test; **Figure 1b**). Also, after the tissue effect was removed by standardisation, principal components
119 analysis (PCA) showed a strong influence of age on the first two PCs, which explains 31% of the
120 variance in total (**Figure 1-figure supplement 2**). We further observed higher similarity among tissues
121 at the juvenile stage compared to the young-adult stage. In other words, distances between tissues
122 increased with age (change in mean Euclidean distance among tissues with age during development
123 in PC1-PC4 space $\rho_{\text{dev}} = 0.99$, $p_{\text{dev}} = 1.5 \times 10^{-5}$, **Figure 1-source data**), which resonates with previous
124 reports of inter-tissue transcriptome divergence during development (Cardoso-Moreira et al. 2019). This
125 divergence pattern was also observed when PCA was performed with developmental samples only
126 (days 2 to 61: change in mean Euclidean distance among tissues in PC1-PC4 space; $\rho = 0.95$, $p = 0.0008$;
127 **Figure 1-figure supplement 3a-b**).

128
129 **Tissues involve common gene expression changes with age.** We next characterised age-related
130 changes in gene expression shared across tissues by i) studying overall trends at the whole
131 transcriptome level and testing their consistency using permutation tests, and ii) studying statistically
132 significant changes at the single gene level. First, we investigated similarities in overall trends of gene
133 expression changes with age using the Spearman's correlation coefficient (ρ) between expression
134 levels and age, for each gene, in each tissue, separately for the developmental and ageing periods
135 (Methods; tissue-specific age-related gene expression changes and functional enrichment test results
136 are available as **Supplementary File 1**). We then examined transcriptome-wide similarities across
137 tissues during development and ageing by comparing these gene-wise expression-age correlation
138 coefficients (**Figure 1c**). Considering the whole transcriptome without a significance cutoff, we found a
139 weak correlation of age-related expression changes in tissue pairs, both during development ($\rho = [0.17,$
140 $0.39]$, permutation test $p < 0.05$ for all the pairs, **Figure 1-source data**), and ageing ($\rho = [0.23, 0.33]$,
141 permutation test $p < 0.05$ in 4/6 pairs, **Figure 1-source data**). We then tested whether developmental

142 patterns among tissues may be shared more than ageing-associated patterns, but we did not find
143 significant difference between inter-tissue similarities within the development and those within ageing
144 (Wilcoxon signed-rank test, $p=0.31$). Moreover, the number of genes with the same direction of change
145 (without applying a significance cutoff) across four tissues was consistently more than expected by
146 chance (permutation test $p<0.05$), except for genes upregulated in ageing (**Figures 1e, Figure 1-figure**
147 **supplement 4**). This attests to overall similarities across tissues both during postnatal development
148 and during ageing, albeit of modest magnitudes. We obtained similar results using another
149 normalisation approach, variance stabilising transformation or VST from the DESeq2 package (Love
150 et al. 2014), and confirmed that the observed patterns are not affected by the choice of normalisation
151 method (**Figure 1-figure supplement 10-11**).

152
153 In the second approach, we focused on genes showing a significant age-related expression change,
154 identified separately during development or during ageing (using Spearman's correlation coefficient and
155 false-discovery rate (FDR) corrected p -value <0.1 , **Figure 1d**). We found that the developmental period
156 was accompanied by a large number of significant changes ($n=[1,941, 6,151]$, 13-41% across tissues),
157 with the most manifest changes detected in the cortex. The genes displaying significant developmental
158 changes across all four tissues also showed significant overlap (**Figure 1-figure supplement 5a,**
159 **Figure 1-figure supplement 6**; permutation test: $p_{\text{shared_up}}=0.027$, $p_{\text{shared_down}}<0.001$). Using the Gene
160 Ontology (GO), we found that shared developmentally up-regulated genes were enriched in functions
161 such as hormone signalling pathways and lipid metabolism (FDR-corrected p -value <0.1). Meanwhile,
162 shared developmentally down-regulated genes were enriched in functions such as cell cycle and cell
163 division (FDR-corrected p -value <0.1 ; **Supplementary File 2**). Contrary to widespread expression
164 change during development (13-41%), the proportion of genes undergoing significant expression
165 change during ageing was between 0.013-15% (**Figure 1d**). This contrast between postnatal
166 development and ageing was also observed in previous work on the primate brain (Somel et al. 2010;
167 Işıldak et al. 2020). In terms of the number of genes with a significant ageing-related change, the most
168 substantial effect we found was in the lung ($n=2,319$), while close to no genes showed a statistically
169 significant change in the muscle ($n=2$), a tissue previously noted for displaying a weak ageing
170 transcriptome signature across multiple datasets (Turan et al. 2019). Not unexpectedly, we found no
171 common significant ageing-related genes across tissues (**Figure 1-figure supplement 5a**).

172 Considering the similarity between the ageing and development datasets (**Figure 1c**) and the similar
173 sample sizes in development (n=7) and ageing periods (n=9), the lack of overlap in significant genes in
174 ageing might be due to low signal-to-noise ratios in the ageing transcriptome, as ageing-related
175 changes are subtler compared to those in development (**Figure 1-figure supplement 5b**).

176

177 **Gene expression reversal is a common phenomenon in multiple tissues.** We then turned to
178 investigate the prevalence of the reversal phenomenon (*i.e.* an opposite direction of change during
179 development and ageing) across the four tissues. We first compared the trends of age-related
180 expression changes between development and ageing periods in the same tissue, without a
181 significance cutoff, to assess transcriptome-wide reversal patterns (**Figure 1c**). This revealed weak
182 negative correlation trends in liver and muscle (though not in the lung and cortex), *i.e.* genes up- or
183 down-regulated during development tended to be down- or up-regulated during ageing, respectively.
184 These reversal trends were comparable when the analysis was repeated with the genes showing
185 relatively high levels of age-related expression change ($|\rho| > 0.6$ in both periods; **Figure 1-figure**
186 **supplement 7**). We further studied the reversal phenomenon by classifying each gene expressed per
187 tissue (n=15,063) into those showing up- or down-regulation during development and during ageing.
188 Here, again, we did not use a statistical significance cutoff and summarised trends of continuous change
189 versus reversal in each tissue. This approach follows Dönertaş et al. (2017) and focuses on global
190 trends instead of single genes. In line with the above results, as well as earlier observations in the brain,
191 kidney, and liver (Dönertaş et al. 2017; Anisimova et al. 2020), we found that ~50% (43-58%) of
192 expressed genes showed reversal trends (**Figure 1f**), although these proportions were not significantly
193 more than randomly expected in permutation tests (**Figure 1-figure supplement 8**, Methods). Overall,
194 we conclude that although the reversal pattern is not ubiquitous, the expression trajectories of the genes
195 do not necessarily continue linearly into the ageing period.

196

197 **Pathways related to development, metabolism and inflammation are associated with the**
198 **reversal pattern.** We then asked whether genes displaying reversal patterns in each tissue may be
199 enriched in functional categories. Our earlier study focusing on different brain regions had revealed that
200 up-down genes, *i.e.* genes showing developmental up-regulation followed by down-regulation during
201 ageing, were enriched in tissue-specific pathways, such as neuronal functions (Dönertaş et al. 2017).

202 Analysing up-down genes compared to all genes up-regulated during development, we also found
203 significant enrichment (FDR corrected p -value <0.1) in functions such as “synaptic signaling” in the
204 cortex, as well as “tube development” and “tissue morphogenesis” in the lung, “protein catabolic
205 process” in the liver and “cellular respiration” pathways in the muscle (**Supplementary File 3**).
206 Meanwhile, down-up genes (down-regulation during development followed by up-regulation during
207 ageing) showed significant enrichment in functions such as “wound healing”, and “peptide metabolic
208 process” in the cortex, “translation” and “nucleotide metabolic process” in the lung, “inflammatory
209 response” in the liver and ‘leukocyte activation’ in the muscle (**Supplementary File 3**).

210
211 **Genes showing a reversal pattern are not shared among tissues.** As tissues displayed modest
212 positive correlations in their development- or ageing-related expression change trends (**Figures 1c**,
213 **Figure 1-figure supplement 7**), and as we had previously observed that distinct brain regions show
214 similarities in their reversal patterns (*i.e.* the same genes showing the same reversal type), different
215 tissues might also be expected to show similarities in their reversal patterns. Interestingly, we found no
216 overlap between gene sets with the reversal pattern (up-down or down-up genes) across tissues,
217 relative to random expectation (permutation test, $p_{\text{up-down}}=0.08$, $p_{\text{down-up}}=0.53$; **Figure 1-figure**
218 **supplement 9**). Such a lack of overlap might be explained if genes showing reversal patterns in each
219 tissue tend to be tissue-specific. It would also be consistent with the notion that reversals involve loss
220 of cellular identities gained in development, during which tissue transcriptomes appear to diverge from
221 each other (**Figures 1a**, **Figure 1-figure supplement 3**) (Cardoso-Moreira et al. 2019). This result led
222 us to ask whether, in accordance with the reversal phenomenon, inter-tissue transcriptome divergence
223 may be followed by increasing inter-tissue similarity, or convergence, during ageing.

224
225 **Inter-tissue divergence during development and convergence during ageing.** We studied the
226 inter-tissue divergence/convergence question using two approaches. In the first, we analysed how
227 transcriptome-wide expression variation among tissues changes with age regardless of their age-
228 related expression patterns in any particular tissue. To do this, for each individual, we calculated the
229 **c**oefficient **o**f **v**ariation (CoV) across the four tissues for each commonly expressed gene ($n=15,063$),
230 which represents a measure of expression variation among tissues. Then, we assessed how such inter-
231 tissue variation changes over the lifetime, by calculating the Spearman’s correlation coefficient between

232 CoV and age, separately for development and ageing periods (correlation values for all genes are given
233 in **Figure 2-source data**).

234

235 Using the CoV values calculated across all 15,063 genes (excluding one 904 days-old individual for
236 which we lacked the cortex data), we observed a significant mean CoV increase in development
237 (Spearman's correlation coefficient $\rho=0.77$, two-sided $p=0.041$), confirming that tissues diverge as
238 development progresses (**Figure 2a**). Interestingly, during ageing, we observed a decrease in mean
239 CoV with age, albeit not significant ($\rho=-0.50$, $p=0.204$, **Figure 2a**), suggesting that tissues may tend to
240 converge during ageing. This was also supported by the PCA analysis in which we observed a trend of
241 ageing-associated decrease in mean Euclidean distance among tissues (using PC1-PC4 space with
242 quantile normalised data: $\rho=-0.87$, $p=0.0026$; with VST normalised data $\rho=-0.58$, $p=0.102$, **Figure 1-**
243 **source data**). We obtained the same divergence-convergence pattern by calculating the median CoV
244 values for each individual instead of the mean (**Figure 2-figure supplement 1**). Figure 2b exemplifies
245 this pattern of increasing and then decreasing CoV through lifetime for the gene displaying the strongest
246 such signal.

247

248 We identified $n=9,058$ genes showing divergent trends among tissues in development based on their
249 CoV change with age (without using a significance cutoff per gene). Among these, $n=4,802$ showed
250 convergent trends in ageing, which we refer to as **divergent-convergent** (DiCo) genes. We next studied
251 the transition points between divergence and convergence by clustering genes showing the DiCo
252 pattern ($n=4,802$) based on their CoV values (**Figure 2-figure supplement 2**). Notably, Cluster 1, which
253 shows a slightly delayed divergence starting after 8-days and peaks around 3-months, was associated
254 with metabolic and respiration-related processes (FDR-corrected $p\text{-value}<0.1$), and Cluster 5, which
255 shows a relatively delayed convergence after 4 months, was enriched in categories related to vascular
256 development (FDR-corrected $p\text{-value}<0.1$) (**Supplementary File 4**). To assess the contribution of
257 different tissues to the DiCo pattern, we further clustered DiCo-displaying genes ($n=4,802$) based on
258 their expression levels (**Figure 2-figure supplement 3**). Not surprisingly, the clusters with relatively
259 higher expression levels of a tissue (e.g. muscle in Cluster 9) were enriched in functional categories
260 (FDR-corrected $p\text{-value}<0.1$) related to that tissue (e.g. muscle cell development) (**Supplementary File**
261 **5**).

262 We then studied DiCo at the single-gene level. We tested each gene for a significant CoV change in
263 their expression levels (*i.e.* divergence or convergence) in development and ageing (Spearman's
264 correlation test with FDR corrected p -value <0.1). We found that the ratio of divergent and convergent
265 genes differed significantly between development (70% divergence among 2,581 significant genes) and
266 ageing (68% convergence among 62 significant genes) (**Figure 2d-e**). The same pattern was also
267 observed without using significance cutoff (**Figure 2-figure supplement 4**). We also confirmed that this
268 pattern is also observed with VST-normalised data (Methods), and is thus not affected by the data
269 preprocessing approach (**Figure 2-figure supplement 14**).

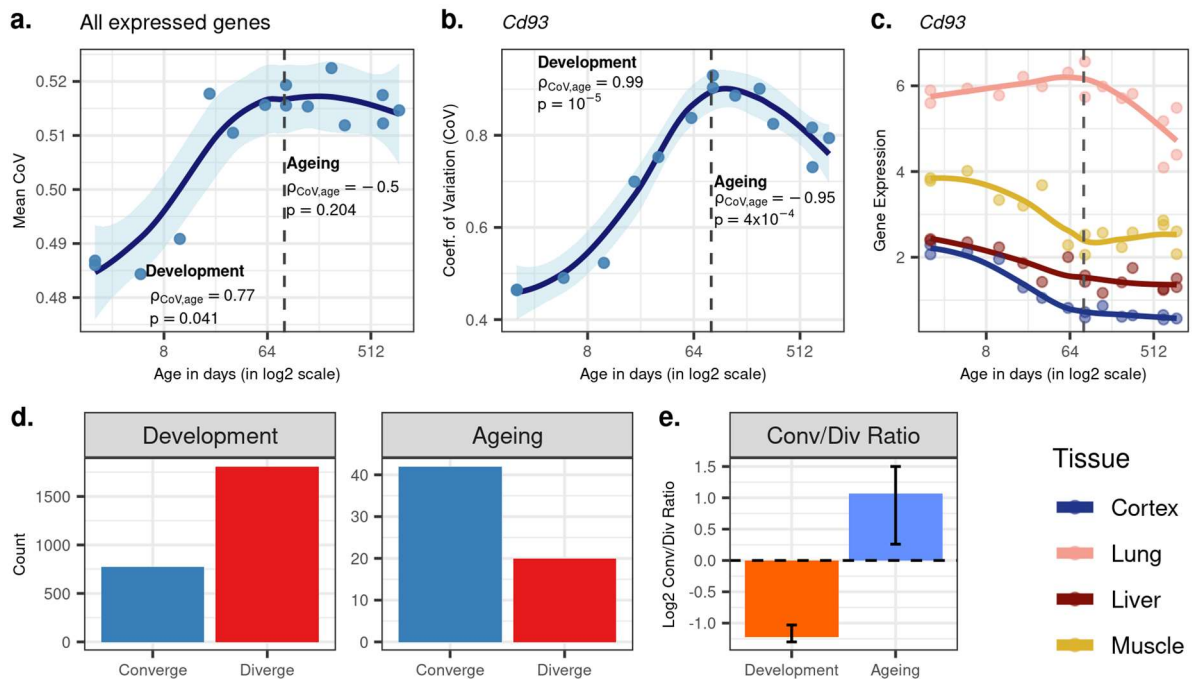
270

271 To our knowledge, inter-tissue convergence during ageing is a novel phenomenon. We first considered
272 the possibility that convergence during ageing could be explained by heteroscedasticity which could
273 arise due to increased inter-individual variability in gene expression during ageing (Somel et al. 2006).
274 To test this hypothesis, we compared expression-age heteroscedasticity levels between two gene sets;
275 1) genes with the DiCo pattern, 2) genes showing divergent patterns throughout lifetime (DiDi, $n=4,182$)
276 for each tissue, separately (Methods). We did not observe any significant difference in
277 heteroscedasticity between DiCo and DiDi genes in any of the tissues (two-sided KS test, $p>0.05$ in all
278 tissues, **Figure 2-figure supplement 15**), which suggests that heteroscedasticity due to increased
279 inter-individual variability probably does not drive the observed age-related convergence during ageing.
280 Visual inspection of gene expression clusters also suggested that the DiCo pattern is not particularly
281 associated with non-linear changes in gene expression with age (**Figure 1-figure supplement 12-15**).

282

283 In order to further verify the DiCo pattern, we used a second approach to test it in our mouse dataset.
284 For each individual, we calculated correlations between pairs of tissues across their gene expression
285 profiles. Under the DiCo pattern, we would expect pairwise correlations to decrease during development
286 and increase during ageing. Among all pairwise comparisons, we observed a strong negative
287 correlation during development ($\rho=[-0.61, -0.9]$, nominal $p<0.05$ in 5 out of 6 tests), while during ageing,
288 4 out of 6 comparisons showed a moderate positive correlation ($\rho=[0.16, 0.69]$, nominal $p<0.05$ in 1 out
289 of 6 comparisons, **Figure 2-figure supplement 5**). Calculating the mean of pairwise correlations among
290 tissues for each individual, we observed the same DiCo pattern (nominal $p<0.05$ for both periods,
291 **Figure 2-figure supplement 6**).

292 **Figure 2. Age-related change in gene expression variation among tissues estimated with CoV**



293

294 **a)** Transcriptome-wide mean CoV trajectory with age. Each point represents the mean CoV value of all protein-

295 coding genes (15,063) for each mouse ($n=15$) except the one that lacks expression data in the cortex. **b)** Age effect

296 on CoV value of the Cd93 gene which has the highest rank for the DiCo pattern, in four tissues (Methods). CoV

297 increases during development and decreases during ageing, indicating expression levels show DiCo patterns

298 among tissues. **c)** Expression trajectories of the gene Cd93 in four tissues. **d)** The number of significant CoV

299 changes with age (FDR corrected p -value <0.1) during development (left, $n_{\text{conv.}}=772$, $n_{\text{div.}}=1,809$) and ageing (right,

300 $n_{\text{conv.}}=42$, $n_{\text{div.}}=20$). Converge: genes showing a negative correlation (ρ) between CoV and age; Diverge: genes

301 showing a positive correlation between CoV and age. **e)** Log2 ratio of convergent/divergent genes in development

302 and in ageing. The graph represents only genes showing significant CoV changes (FDR corrected p -value <0.1 ,

303 given in panel d). Error bars represent the range of log2 ratios calculated from leave-one-out samples using the

304 jackknife procedure (Methods, values are given in **Figure 2-source data**).

305

306

307

308

309

310

311

312 **The divergence-convergence (DiCo) pattern indicates loss of tissue-specificity during ageing.**

313 Potential explanations of the DiCo pattern involve two scenarios consistent with the age-related loss of
314 identity: i) decreased expression of tissue-specific genes in their native tissues, or ii) non-specific
315 expression of tissue-specific genes in other tissues. To test these predictions, we first identified tissue-
316 specific gene sets based on relatively high expression of that gene in a particular tissue (cortex: 1,175,
317 lung: 839, liver: 986, muscle: 766 genes). We noted that tissue-specific genes show clear up-down
318 reversal patterns, being mostly up-regulated during development, and down-regulated during ageing
319 (**Figure 3**, 57-89%). The up-down reversal pattern was particularly strong among tissue-specific genes
320 for the three of four tissues tested (OR = [1.65, 6.52], $p < 0.05$ for each tissue except in liver: OR=0.87,
321 $p=0.09$, **Figure 3-source data**). Tissue-specific genes were also enriched among DiCo genes (**Figure**
322 **3-source data**, OR=1.56, Fisher's exact test $p < 10^{-16}$).

323

324

325

326

327

328

329

330

331

332

333

334

335

336

337

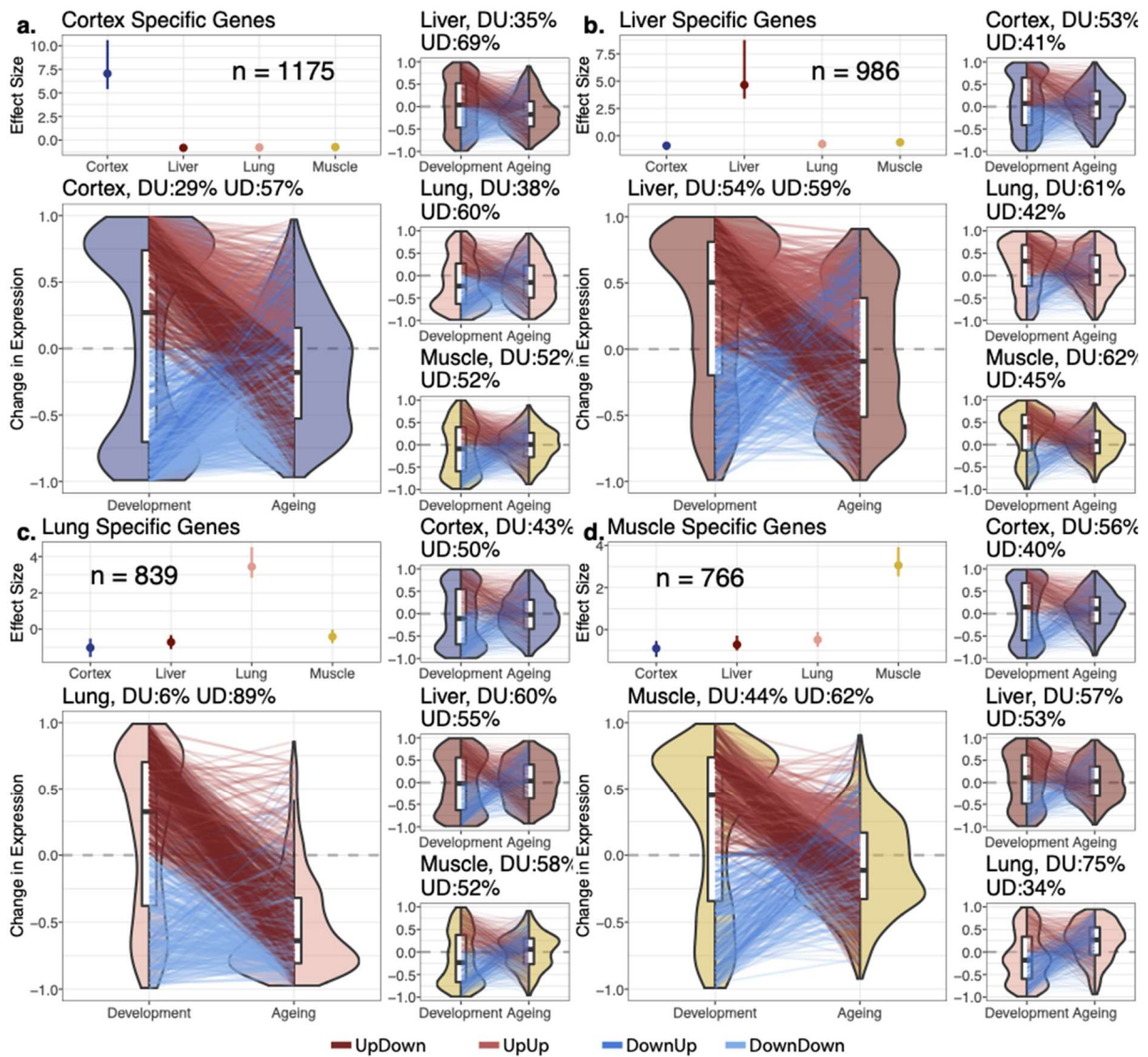
338

339

340

341

342 **Figure 3. Reversal patterns among tissue-specific genes**



343

344 Age-related expression changes of the tissue-specific genes. In each panel **a-d**, the upper left subpanels show
 345 effect size (ES) calculated with the Cohen's D formula, using expression levels of each gene among tissues
 346 (Methods). The IQR (line range) and median (point) effect size for each tissue is shown. The number of tissue-
 347 specific genes is indicated inside each subpanel. The lower left subpanels show violin plots of the distribution of
 348 age-related expression change values (Methods) among tissue-specific genes, in development and in ageing. Each
 349 quadrant represents the plots for each tissue-specific gene group. The red and blue lines connect gene expression
 350 changes for the same genes in development and ageing. DU: percentage of down-up reversal genes among down-
 351 regulated, tissue-specific genes in development. UD: percentage of up-down reversal genes among up-regulated,
 352 tissue-specific genes in development. Tissue-specific genes are enriched among UD reversal genes except in the
 353 liver (Fisher's exact test; $OR_{cortex}=1.65$, $OR_{lung}=6.52$, $OR_{liver}=0.87$, $OR_{muscle}=1.26$, $p<0.05$ for each test except in
 354 liver).

355 We then tested our initial prediction that the DiCo pattern is related to tissue-specific genes losing their
356 expression in their native tissue and/or gaining expression in non-native tissues during ageing. We first
357 tested this hypothesis by considering all tissue-specific genes. We found a positive odds ratio between
358 loss of expression in native tissue and gain in other tissues during ageing (OR = 5.50, Fisher's exact
359 test $p=2.1 \times 10^{-129}$, **Figure 4a**). The same analysis conducted with only the DiCo genes yielded a much
360 stronger association (OR=74.81, Fisher's exact test $p=5.9 \times 10^{-203}$, **Figure 4b**). This suggests that loss
361 of tissue-specific expression is observed across the transcriptome, with a particularly strong association
362 among DiCo genes. Figure 4c-f exemplifies the expression trajectories of genes chosen from each
363 group defined in Figure 4b.

364

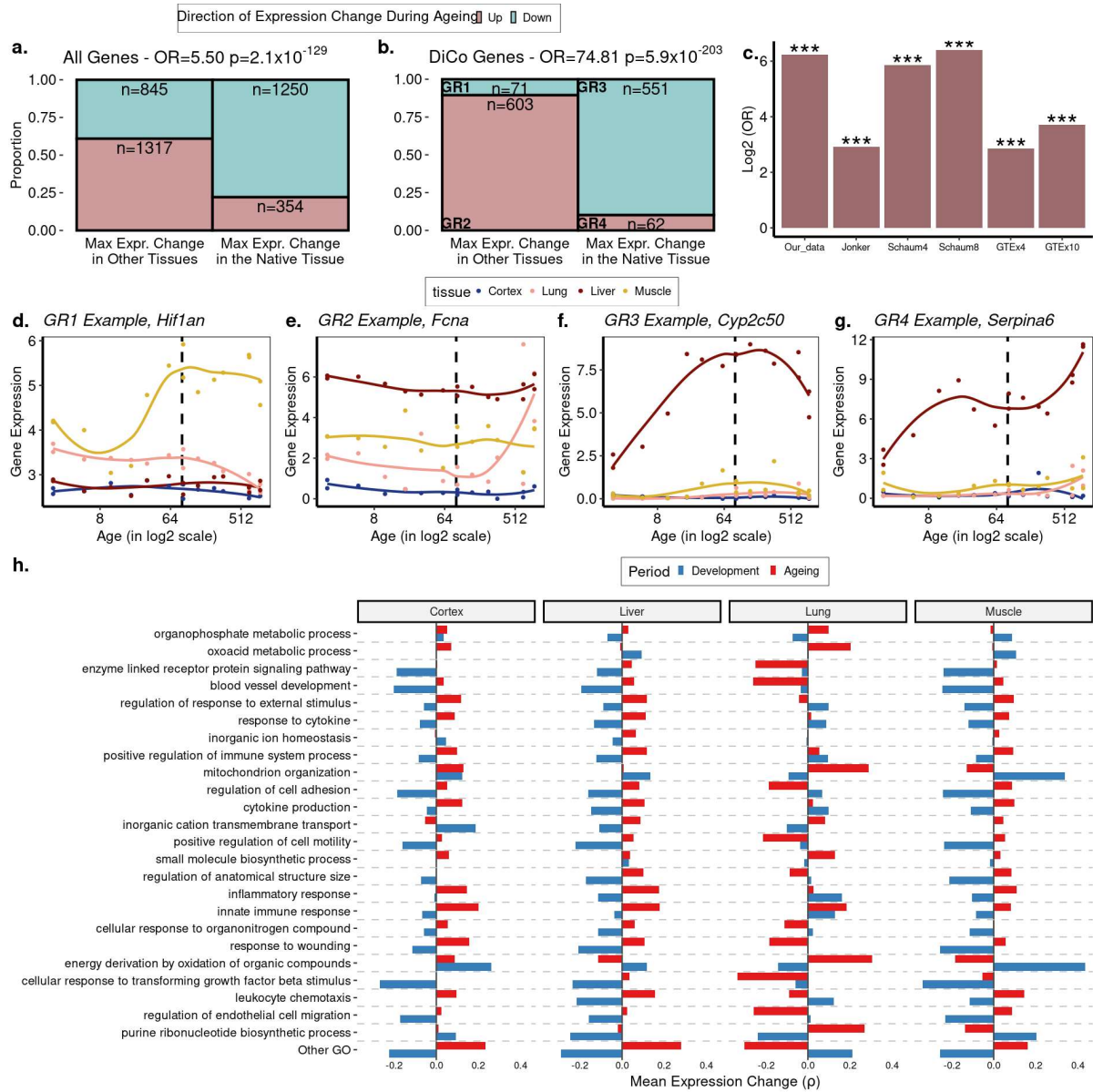
365 We then asked whether genes displaying the DiCo pattern may be related to specific functional
366 pathways or share specific regulators. Using GO, we searched for functional enrichment among
367 convergent genes during ageing, using developmentally divergent genes as the background (Methods).
368 We found enrichment for 184 GO **B**iological **P**rocess (BP) categories for the DiCo pattern (**K**olmogorov-
369 **S**mirnov (KS) Test, FDR-corrected p -value <0.1 , **Figure 4-source data**) and summarised enriched
370 categories by clustering them based on the number of genes they share. We then studied the trends of
371 gene expression changes with age (without a significance cutoff) in each representative category for
372 each tissue (Methods) (**Figure 4h**; we provide detailed clustering for the categories in 'Other GO'
373 (**Figure 4-figure supplement 1**)). On average, energy metabolism, mitochondria and tissue function-
374 related categories, as well as immune response-related categories, exhibit DiCo type expression
375 changes over time and across tissues, where temporal changes in different tissues occur in opposite
376 directions. Notably, for the majority of representative GO categories, the lung had the most distinct
377 expression patterns in both periods (**Figure 4h**, **Figure 4-figure supplement 1**).

378

379 Contrary to the functional enrichment results, we did not find any specific regulators (miRNA or
380 transcription factors) associated with DiCo using the same background as above (at 235 tests for
381 miRNA and 158 tests for TF, FDR corrected p -value >0.1 for both tests) (Methods), which suggests that
382 DiCo pattern may not be driven by a limited number of specific regulators, but may instead be a
383 transcriptome-wide phenomenon.

384

385 **Figure 4. The loss of tissue-specific expression during ageing and functional enrichment of DiCo**
 386 **genes**



387
 388 **a)** Mosaic plot showing the association between maximal expression change in native vs. non-native tissues (x-
 389 axis) vs. down- (cyan) or up- (pink) regulation during ageing across all tissue-specific genes (n=3,766). The highly
 390 significant odds ratio indicates that genes native to a tissue tend to be down-regulated during ageing in that native
 391 tissue, if they show maximal expression change during ageing in that tissue. Conversely, if they show maximal
 392 expression change during ageing in non-native tissue, those genes are up-regulated during ageing. Consequently,
 393 tissue-specific expression patterns established during development will tend to be lost during ageing. **b)** The same
 394 as (a) but using only the tissue-specific genes that show the DiCo pattern (n=1,287). **c)** Summary of the association
 395 tests for 'direction of maximal expression change in native vs. non-native tissues' across all datasets analysed.
 396 The y-axis shows \log_2 transformed Odds Ratio (OR) for each dataset (x-axis) - Schaum4: using the same four

397 *tissues as our dataset. Schaum8: using eight tissues. GTEx4: using the same four tissues as our dataset. GTEx10:*
398 *using ten tissues. ***: FDR-corrected p -value $< 10^{-87}$. P -values are given in **Table 1**. The 4 groups are annotated as*
399 *GR1-4 and gene expression changes for each group in our dataset is exemplified in **d-g. h**) Trends of expression*
400 *change with age of genes (x -axis) in categories enriched in DiCo (GSEA). Enriched categories ($n=184$) are*
401 *summarised into representatives (y -axis) using hierarchical clustering and Jaccard similarities (Methods).*
402 *Categories are ordered by the number of genes they contain from highest (bottom, $n = 290$) to lowest (top, $n = 26$).*
403 *The most distant cluster with low within-cluster similarity in the hierarchical clustering (Other GO) was clustered*
404 *separately and given in **Figure 4-figure supplement 1**.*

405

406 **Additional mouse and human datasets confirm the association between loss of tissue-**
407 **specificity and inter-tissue convergence during ageing.** We investigated inter-tissue convergence
408 during ageing in three additional datasets where multiple tissue samples were available for the same
409 individuals (**Table 2**). We conducted the analysis using a subset of the same four tissues in our dataset
410 and also larger sets when additional samples were available. Age-related expression changes showed
411 small to moderate correlations among all datasets analysed, with our dataset being most similar to the
412 mouse dataset from Jonker et al., while the GTEx human dataset was the most distinct (**Figure 4-figure**
413 **supplement 2a**).

414

415 First, using the Jonker et al. dataset (Jonker et al. 2013) comprising 5 tissues (**Table 2**), we observed
416 transcriptome-wide convergence during ageing with a significant decline in mean Euclidean distance
417 between PCs ($\rho = -0.57$, $p = 0.014$, **Figure 2-figure supplement 7a-c**) and a strong decrease in mean
418 CoV during ageing ($\rho = -0.48$, $p = 0.044$, **Figure 2-figure supplement 7d**). Moreover, we found that
419 7/10 tissue pairs showed increased pairwise tissue correlations during ageing, although none of them
420 was significant after multiple testing correction (**Figure 2-figure supplement 7f**). Sixty-six percent of
421 the genes with a significant change in CoV were convergent, comparable to our dataset showing 68%
422 convergence among significant changes. We also tested the association between the loss of identity
423 and convergence pattern by repeating the same analysis as in Figure 4b with the Jonker et al. dataset,
424 using only the convergent genes in ageing as we lack developmental period. We again found strong
425 association, consistent with convergent genes losing expression in their native tissue and gaining in
426 other tissues during ageing (OR=7.52, $p < 10^{-16}$, **Figure 4c**). The results are summarised in **Table 1**.

427

428 Next, we used another mouse dataset by Schaum et al. (Schaum et al. 2020) (**Table 2**). Repeating the
429 analysis on the same 4 tissues and also a larger set of 8 tissues, we did not find support for
430 transcriptome-wide convergence (**Table 1, Figure 2-figure supplement 17, 19**). In the 4-tissue
431 comparison 4/6 tissue-pairs, and in the 8-tissue comparison only 16/28 tissue-pairs showed positive
432 correlations, supporting the inter-tissue convergence during ageing (**Figure 2-figure supplement 18c,**
433 **20c**). Interestingly, 75% of the negative correlations involved muscle and subcutaneous fat.
434 Convergence ratios among genes showing significant change in CoV (FDR corrected p -value <0.1) were
435 marginally above 50%. Although we did not observe widespread convergence during ageing in this
436 dataset, we still detected strong associations between convergence in ageing and tissue specificity
437 ($OR_{4\text{-tissue}}=1.33$, $p = 1.08 \times 10^{-8}$) and identity loss ($OR_{4\text{-tissue}}=58.3$ $p < 10^{-16}$; $OR_{8\text{-tissue}}=84.2$ $p < 10^{-16}$)
438 (**Figure 4c**).

439
440 Lastly, we used the GTEx dataset to investigate inter-tissue convergence during ageing in humans.
441 Calculating the change in mean Euclidean distance based on PCA and mean CoV values, we found a
442 non-significant tendency towards convergence across the whole transcriptome in the same 4 tissues
443 and a larger set of 10 tissues (**Table 1, Figure 2-figure supplement 8, 10**). We also performed the 4-
444 tissue comparison with female and male individuals separately and observed relatively strong inter-
445 tissue convergence among ageing females ($\rho_{\text{female}} = -0.58$, $p_{\text{female}} = 0.059$) but less in males ($\rho_{\text{male}} = -0.052$,
446 $p_{\text{male}} = 0.77$) which lack individuals at the youngest and oldest age groups (**Figure 2-figure supplement**
447 **16**). Moreover, 5/6 and 29/45 tissue-pairs showed increased correlation with age in 4-tissue and 10-
448 tissue comparisons, consistent with inter-tissue convergence during ageing (**Figure 2-figure**
449 **supplement 9, 11**). Notably, 8 of 16 negative correlations in the 10-tissue comparison involved the skin
450 tissue (**Figure 2-figure supplement 11c**). We also studied significant changes in CoV per gene, but
451 found no significant gene in the 4-tissue comparison and only 3 genes in the 10-tissue comparison, all
452 of which were convergent. Finally, we tested the association between the loss of expression in native
453 tissue and gain in other tissues during ageing among convergent genes, confirming the association with
454 the tissue identity (**Figure 4c, Table 1**).

455
456 Overall, analysis of these three additional datasets indicates that inter-tissue convergence during
457 ageing is commonly, but not always, observed at the transcriptome-wide level in mice and in humans.

458 Notably, the transcriptome-wide trend was weak in the Jonker et al. and GTEx datasets and not evident
459 in the Schaum et al. dataset. The association between the loss of identity and convergence, on the
460 other hand, was strong across all datasets (**Table 1**).

461

462 We further asked whether convergent gene sets identified in different datasets overlap. Eleven of 15
463 comparisons were significant, but the effect sizes were small (**Figure 4-figure supplement 2b**). We
464 reason that the low overlap across datasets might reflect that transcriptome-wide convergence was
465 weak and that we lack the developmental samples for the external datasets, *i.e.* we can only compare
466 convergence during ageing but not the DiCo pattern. Noteworthy, only 62% of convergent genes in
467 ageing are divergent during development in our dataset, and low overlap between convergence does
468 not rule out overlap across DiCo genes.

469

470 These results suggest that inter-tissue convergence in ageing may be a weak but widespread
471 phenomenon and associated with the loss of tissue identity. Overall, while mouse and human tissues
472 display divergence in development (**Figures 1a, 2a, (Cardoso-Moreira et al. 2019)**), this appears to be
473 followed by a trend towards inter-tissue convergence in ageing (**Figures 2a, Figure 2-figure
474 supplement 1-20**), and could be linked to loss of tissue identity.

475

476 **Table 1:** Result summary of the all datasets analysed. First column shows the names of datasets analysed.
477 Numbers in parentheses show the sample sizes. 'Among all genes' column refers to the analyses performed using
478 all genes relevant to those analyses (subcolumns) without a significance cutoff. 'Within significant CoV changes':
479 genes show significant CoV change with age with FDR corrected p-value<0.1. In the 'DiCo vs Tissue specificity
480 (Di- as background)' column, divergent genes in development (Di-) were chosen as background. 'Co vs expression
481 change in native tissue association (Fig 4b)' column refers to the analysis performed in Figure 4b for each dataset
482 and the results were presented in Figure 4c. The association tests were performed among convergent genes in
483 ageing except in our dataset which was performed with DiCo genes. Significant test results were indicated with
484 bold fonts. Green cells show the results that support convergence or tissue-specific expression loss in ageing
485 whether as a significant result or as a trend. Unsupportive test results and inapplicable tests were coloured grey
486 and light yellow, respectively. rho: Spearman's correlation coefficient. OR: Odds ratio. * FDR corrected p-value<0.1.

487

	Among all genes						Within significant CoV changes
	PCA Change in Euclidean distance	Mean CoV change	Median CoV change	Pairwise tissue correlations	DiCo vs tissue specificity (Di- as background)	Co vs expression change in native tissue association (Fig 4b)	Co vs. Di proportions
Izgi2021	rho=-0.87, p=0.0026	rho=-0.5, p=0.2	rho=-0.48, p=0.23	4/6 positive, none significant*	OR=1.56, p=1.3x10⁻¹⁸	OR=74.81 p=5.9x10⁻²⁰³ (among 1287 DiCo genes)	68% convergence (among 62 significant genes*)
Jonker2013 5 tissues, 2 different than ours (n=18)	rho=-0.57, p=0.014	rho=-0.48, p=0.044	rho=-0.03, p=0.91	7/10 positive, none significant*	Di-background missing	OR=7.52, p=6.5x10⁻¹⁰⁹ (among 2967 convergent genes)	66% convergence (among 1735 significant genes*)
Schaum2020 Same 4 tissues (n=37)	rho=0.13, p=0.46	rho=0.25, p=0.14	rho=0.13, p=0.43	4/6 positive, 2 significant*	OR=1.33, p=1.07x10⁻⁸	OR=58.03, p=1.5x10⁻¹⁹⁷ (among 2124 convergent genes)	53% convergence (among 319 significant genes*)
Schaum2020 8 tissues (n=26)	rho=0.1, p=0.62	rho=0.16, p=0.43	rho=0.04, p=0.86	16/28 positive, 5 significant*	Di-background missing	OR=84.2, p=9.7x10⁻⁹⁶ (among 2380 convergent genes)	54% convergence (among 244 significant genes*)
GTEx Same 4 tissues	rho=-0.23, p=0.12	rho=-0.12, p=0.42	rho=-0.18, p=0.23	5/6 positive, none significant*	Di-background missing	OR=7.21, p=7x10⁻⁸⁷ (among 2407 convergent genes)	(no significant CoV changes)
GTEx 10 tissues	rho=-0.26, p=0.13	rho=-0.14, p=0.44	rho=-0.3, p=0.08	29/45 positive, none significant*	Di-background missing	OR=13.01, p=5.7x10⁻¹¹⁴ (among 2195 convergent genes)	(all 3 significant genes were convergent)

488

489

490

491

492

493

494

495

496

497

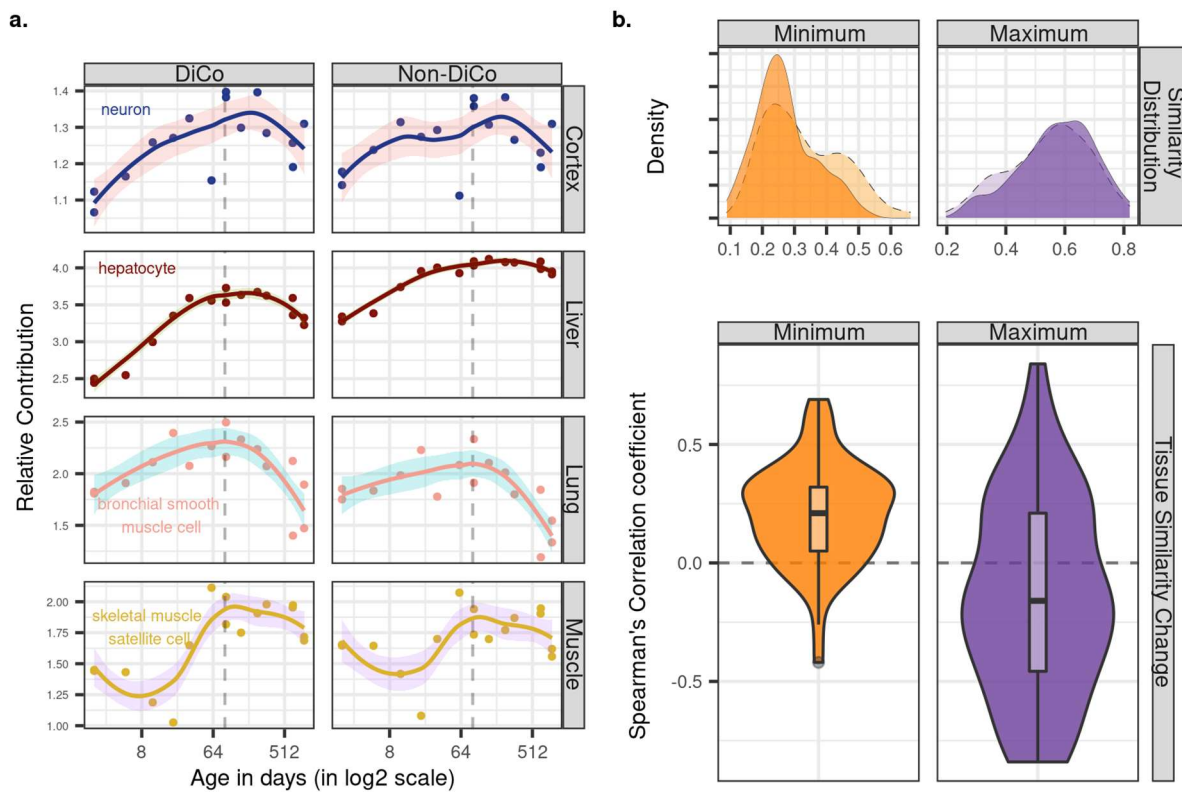
498 **Changes in cellular composition and cell-autonomous expression can both explain the**
499 **divergence-convergence pattern.** Ageing-related transcriptome changes observed using bulk tissue
500 samples may be explained by temporal changes in cell type proportions within tissues, by cell-
501 autonomous expression changes, or both. To explore whether the observed inter-tissue DiCo patterns
502 may be attributed to changes in cell type proportions, we used published data from a mouse single-cell
503 RNA-sequencing experiment (Tabula Muris Consortium 2020). For each of the four tissues in our
504 original experiment, we collected cell type-specific expression profiles from 3-month-old young adult
505 mice in the Tabula Muris Senis dataset. We deconvoluted bulk tissue expression profiles in our mouse
506 dataset using the corresponding tissue's cell type-specific expression profiles by regression analysis
507 (Methods), and studied the relative contributions of each cell type to tissue transcriptomes and how
508 these change with age. The analysis was performed with three gene sets; all genes ($n=[12,492,$
509 $12,849]$), DiCo ($n=[4,007, 4,106]$) and non-DiCo genes ($n=[8,485, 8,743]$). Studying these
510 deconvolution patterns, we observed a weak but consistent trend involving the most common cell types
511 in different tissues. For instance, analysing DiCo genes in the liver and lung, we found that the most
512 common cell type's contribution (hepatocyte in the liver, and bronchial smooth muscle cell in the lung)
513 tends to increase during development (Spearman's correlation coefficient $\rho_{liver}=0.95$, $\rho_{lung}=0.81$, nominal
514 $p<0.05$). This contribution then decreases during ageing ($\rho_{liver}=-0.77$, $\rho_{lung}=-0.86$, nominal $p<0.05$)
515 **(Figure 5a, Figure 5-figure supplement 1)**. This pattern was also observed in muscle and cortex,
516 albeit not significantly **(Figure 5a, Figure 5-figure supplement 1)**. These changes most likely reflect
517 shifts in cellular composition, some of which were demonstrated directly in mice using *in situ* RNA
518 staining (Tabula Muris Consortium 2020). Repeating the analysis with non-DiCo genes resulted in
519 highly similar patterns considering the most common cell types in tissues, except in muscle ageing in
520 which the age-related decrease was significantly higher with DiCo genes than the non-DiCo genes
521 (permutation test with re-sampling all genes, $p_{skeletal-muscle-satellite-cell}=0.04$) **(Figure 5a, Figure 5-figure**
522 **supplement 1, Figure 5-figure supplement 2-5)**. These results indicate that the observed cellular
523 composition changes may partly explain DiCo, although the influence of composition changes is not
524 exclusive to genes displaying the DiCo pattern.

525

526

527

528 **Figure 5. Contribution of tissue composition and cell-autonomous changes to the DiCo pattern**



529

530 **a)** Deconvolution analysis of our mouse dataset with the 3-month-old scRNA-seq data (*Tabula Muris Senis*) using
 531 *DiCo* ($n=[4,007, 4,106]$) and *non-DiCo* ($n=[8,485, 8,743]$) genes. Only the cell types with the highest relative
 532 contributions to each tissue bulk transcriptome are shown (cell type names are given within each plot).
 533 Contributions of all cell types to bulk tissue transcriptomes are shown in **Figure 5-figure supplement 1**. **b)**
 534 Distribution of correlations for minimally (left) and maximally (right) correlated cell type pairs among tissues ($n=54$
 535 pairs). For each cell type of a given tissue, one minimally (or maximally) correlated cell type is chosen from other
 536 tissues among the 3-month age group of the *Tabula Muris Senis* dataset (density plots with solid line edges).
 537 Dashed lines show the correlation distributions in 24-months age of minimally or maximally correlated cell type
 538 pairs identified in the 3-months age group. Bottom panel shows age-related expression similarity (ρ) changes of
 539 minimally (left) and maximally (right) correlated cell type pairs. The correlation between age and tissue similarity
 540 (expression correlations) were calculated for each pair of cell types identified in the 3-months age group. All
 541 pairwise cell type correlations and their age-related changes are given in **Figure 5-source data**.

542

543

544

545

546

547 Next, we investigated the possible role of cell-autonomous changes in the DiCo pattern. Cell-
548 autonomous changes could contribute to inter-tissue convergence during ageing in two ways. First,
549 expression profiles of similar cell types shared across different tissues, such as immune cells, might
550 converge with age. Another possible scenario, consistent with the notion of age-related cellular identity
551 loss, is that the expression profiles of unrelated cell types, such as tissue-specific cell types in different
552 tissues converge with age. To test these scenarios, we first ordered the pairwise correlations between
553 cell types in different tissues at 3 months age group to determine the most similar and dissimilar cell
554 types across tissues (Methods). Then, we studied how these similarities (*i.e.* pairwise correlations)
555 change with age (**Figure 5b**). Intriguingly, we found that pairs of similar cell types (*i.e.* those with the
556 highest correlations) among tissues tend to become less similar with age (36/54 [67%] of pairwise
557 comparisons, **Figure 5-source data**). On the contrary, the most distinct cell types (*i.e.* those with the
558 lowest correlations) among tissues become more similar with age (45/54 [83%], **Figure 5-source data**).
559 Repeating the analysis considering DiCo genes only yielded a similar trend (30/54 [56%] decrease in
560 correlation among the most similar cell types, permutation test with re-sampling non-DiCo genes, $p > 0.1$;
561 and 47/54 [87%] increase in correlation among the most distinct cell types, permutation test, $p > 0.1$).
562 These trends are consistent with age-related cellular identity loss, and they suggest that cell-
563 autonomous changes may also contribute to inter-tissue convergence during ageing, although further
564 data and analyses would be needed to fully establish their validity.

565
566 Finally, we tested the possibility of intra-tissue convergence of cell types in the Tabula Muris Senis
567 dataset, by calculating expression variation among cell types using the CoV measure for each
568 individual. However, we did not observe a consistent trend of increasing similarity among cell types
569 within tissues from 3m- to 24m-old mice (**Figure 5-figure supplement 6**).

570

571 **Discussion**

572 Our findings confirm a number of ageing-associated phenomena identified earlier, while also revealing
573 new patterns. First, we report parallel age-related expression changes among the four tissues studied,
574 during development, as well as in ageing. The inter-tissue correlation distributions were modest and
575 also comparable between development and ageing (**Figure 1c**). This last point may appear surprising
576 at first glance, given the stochastic nature of ageing relative to development (Bahar et al. 2006;

577 Martinez-Jimenez et al. 2017; Angelidis et al. 2019; Somel et al. 2006; Feser et al. 2010; Kim,
578 Villeponteau, and Jazwinski 1996; Enge et al. 2017), and also given earlier observations that
579 developmental expression changes tend to be evolutionarily conserved, while ageing-related changes
580 much less so (Zahn et al. 2007; Somel et al. 2010). At the same time, when we consider that tissues
581 diverge during development, and also that ageing is characterised by parallel expression changes
582 among tissues related to damage response, inflammation, and reduced energy metabolism (Zahn et al.
583 2007; Yang et al. 2015), similar magnitudes of correlations during development and ageing may be
584 expected.

585
586 Second, we verify the generality of the reversal pattern, *i.e.* up-down or down-up expression change
587 patterns across the lifetime, among distinct mouse tissues that include both highly mitotic (lung and
588 liver) and less mitotic ones (skeletal muscle and cortex). Consistent with earlier observations in fewer
589 tissues (Anisimova et al. 2020; Dönertaş et al. 2017), we find that about half the expressed genes
590 display reversal in all cases studied. Importantly, expression reversal is not ubiquitous across all genes
591 and our findings do not necessarily contradict the hyperfunction theory. Instead, we suggest that
592 reversal is a common phenomenon that influences a notable fraction of the transcriptome and is a likely
593 contributor to mammalian ageing.

594
595 Two observations here are notable. One is that reversal-displaying genes, especially those displaying
596 the up-down pattern in each tissue, can be associated with tissue-specialisation-related pathways (*e.g.*
597 morphogenesis) and tissue-specific functions (*e.g.* synaptic activity). The second observation is the lack
598 of significant overlap among reversal genes among tissues. We thus hypothesised that reversals might
599 be reflecting tissue specialisation during development (hence lack of overlap among tissues), and loss
600 of specialisation during ageing. These processes could manifest themselves as inter-tissue divergence
601 and convergence patterns over lifetime. We indeed observed that the up-down reversal pattern is
602 enriched in tissue-specific genes, except in the liver. Studying inter-tissue similarity across mouse
603 lifespan, we further found that the four tissues' transcriptomes diverged during postnatal development,
604 and we further detected a trend towards inter-tissue convergence during ageing. We then further
605 investigated this phenomenon through different approaches: i) by studying overall trends using PCA, ii)
606 by analysing transcriptome-wide trends of inter-tissue CoV without considering gene-wise significance

607 cutoffs, iii) by focusing on genes with significant age-related changes in inter-tissue CoV, iv) by studying
608 age-related changes in pairwise tissue correlations, and v) by analysing different cell-types using
609 scRNA-seq data, and vi) by repeating the same analysis using independent mouse and human ageing
610 datasets. The patterns we found were mostly consistent with inter-tissue convergence, but the majority
611 of transcriptome-wide results were associated with low effect sizes, and some were not statistically
612 significant. Importantly, all significant results suggested convergence during ageing. We therefore
613 conclude that (1) developmental inter-tissue divergence does not continue into ageing; (2) convergence
614 during ageing may be common although possibly not ubiquitous.

615

616 The weakness of the inter-tissue convergence signal per dataset and the limited overlap between
617 convergent gene sets among datasets could have multiple reasons. These include the low signal-to-
618 noise ratios characterising ageing-related expression patterns, the lack of old age individuals in our
619 mouse dataset (>3-year-old mice) and the GTEx dataset (>90-year-old humans), limited overlap of
620 tissues between our mouse dataset (cortex, liver, lung and muscle) and the Jonker et al. dataset (cortex,
621 liver, lung, spleen, kidney), as well as differences in ageing patterns between species or between sexes.
622 Further research involving larger sample sizes and diverse species are needed to confirm the
623 generalisability of the observations.

624

625 Finally, we report a number of interesting observations on DiCo. We determine that tissue-specific
626 genes tend to be down-regulated in the tissues that they belong to during ageing, while non-tissue-
627 specific genes are up-regulated, which was confirmed by all external datasets (**Figure 4c**). Second,
628 using deconvolution, we infer that cell types most common in a tissue (*e.g.* hepatocytes in the liver)
629 tend to increase in frequency during development, but then decrease in frequency during ageing, as
630 also shown recently using immunohistochemistry in a number of mouse tissues (Tabula Muris
631 Consortium 2020). Accordingly, the DiCo phenomenon may at least partly be explained by shifts in
632 cellular composition. This is intriguing as both highly mitotic and low mitotic tissues share this trend,
633 indicating that an explanation based on stem cell exhaustion may not be applicable here. Third, we find
634 increased expression similarity between distinct cell types in different tissues during ageing, but
635 decreased similarity between similar cell types. Cell-autonomous expression changes, therefore, likely
636 also contribute to the divergence-convergence phenomenon. We note that higher expression variability

637 among cells at old age (Hernando-Herraez et al. 2019; Enge et al. 2017) could also lead to inter-tissue
638 convergence during ageing. A fourth interesting observation was the absence of significant enrichment
639 for specific transcription factor or microRNA targets among DiCo genes. This result may not be
640 surprising if inter-tissue convergence is mostly driven by stochastic damage accumulation, such as loss
641 of epigenetic marks. It is also possible that instead of specific regulators, their interaction and
642 cooperativity are associated with the DiCo. Future experimental studies could test both mechanistic
643 aspects and functional link to tissue specificity.

644

645 We also note two major limitations of our study. One is related to the fact that our dataset represents
646 bulk tissue samples, which may suffer from infiltration of foreign cell-types into tissues. Indeed, one of
647 the external datasets, Schaum et al., included samples from perfused mice (Schaum et al. 2020) and
648 we did not find support for the transcriptome-wide convergence during ageing, even though the
649 association between tissue identity loss and convergence was also evident. The scRNA-seq dataset
650 we analysed further suggested that DiCo is associated with tissue-specific genes and not immune- or
651 blood-related categories, but we still cannot rule out possible infiltration artefacts that may affect our
652 results. A second limitation is related to ageing being highly sex-dimorphic in mammals (Yuan et al.
653 2012; Sampathkumar et al. 2020). Hence, in-depth analysis of sex-specificity of the DiCo pattern could
654 be relevant. Our mouse dataset included only male mice, while that of Jonker et al. was female-only.
655 The fact that both revealed DiCo patterns suggest DiCo is not particular to one sex, but there could still
656 exist sex-specific effects. In fact, when we analysed DiCo among human male and female individuals
657 in the GTEx dataset separately, we observed slightly stronger inter-tissue convergence among ageing
658 females than in males, although the GTEx male samples has also a drastically narrower age range
659 **(Figure 2-figure supplement 16)**. Accordingly, the prevalence of DiCo among humans and sexes waits
660 to be determined.

661

662 Despite the open questions that remain, our results consistently support a model where ageing
663 mammals suffer from loss of specialisation at the tissue level, and possibly also at the cellular level,
664 which are observed as expression reversals and the newly discovered divergence-convergence
665 phenomenon we report here.

666

667 **Materials and Methods**

668 **Sample Collection**

669 We collected bulk tissue samples from 16 male C57BL/6J mice. The samples were snap frozen in liquid
670 nitrogen and stored at -80C. No perfusion was applied. The mice were of different ages covering the
671 whole lifespan of *Mus musculus*, comprising both postnatal development and ageing periods. The
672 samples included four different tissues; cerebral cortex, liver, lung and skeletal muscle. One 904 days-
673 old mouse had no cortex tissue sample, and was thus excluded from the analysis. As a result, we
674 generated 63 RNA-seq libraries in total.

675

676 Separation of development and ageing periods:

677 In order to compare gene expression changes during postnatal development and ageing we studied
678 the samples before sexual maturation (covering 2 to 61 days of age, n=7) as the postnatal development
679 period, and samples covering 93 to 904 days (n=9 in all tissues except in cortex where we had n=8) as
680 the ageing period.

681

682 **RNA-Seq Library Preparation**

683 RNA sequencing was performed as previously described (Liu et al. 2016) with slight modifications.
684 Briefly, total RNA was extracted using the Trizol reagent (Invitrogen) from frozen tissue samples. For
685 sequencing library construction, we randomised all samples to avoid batch effects, and used the TruSeq
686 RNA Sample Preparation Kit (Illumina) according to the manufacturer's instruction. Libraries were then
687 sequenced on the Illumina HiSeq 4000 system in three lanes within one flow-cell, using the 150-bp
688 paired-end module.

689

690 **RNA-Seq Data Preprocessing**

691 The quality assessment of the raw RNA-seq data was performed using FastQC v.0.11.5 (Andrews
692 2010). Adapters were removed using Trimmomatic v.0.36 (Bolger, Lohse, and Usadel 2014). The low-
693 quality reads were filtered using the parameters: "PE ILLUMINACLIP: TruSeq3-PE-2.fa:2:30:1:0:8:true,
694 SLIDINGWINDOW:4:15, MINLEN:25". The remaining high-quality reads were aligned to the mouse
695 reference genome GRCm38 using STAR-2.5.3 (Dobin et al. 2013) with parameters: "--sjdbOverhang
696 99 --outSAMattrIHstart 0 --outSAMstrandfield intronMotif --sjdbGTFfile GRCm38.gtf". The percentage

697 of uniquely mapped reads in libraries ranged from 80 to 93%. We used cufflinks v.2.2.1 (Trapnell et al.
698 2010) to generate read counts for uniquely aligned reads (samtools “-q 255” filter) and calculated
699 expression levels as fragment per kilobase million (FPKM). In total, we quantified expression levels for
700 51,608 genes in the GRCm38.gtf GTF file. We identified 50 duplicated genes with 1> FPKM value
701 assigned, and the sum of their FPKM values were used.

702

703 All the remaining analysis was performed in R v.4.1. We restricted the whole analysis to only protein-
704 coding genes obtained by the ‘biotype’ feature of the biomaRt library v.2.48.2 (Durinck et al. 2009). We
705 also excluded genes which were not detected (zero FPKM) in 25% or more of the samples (at least 15
706 of 63), resulting in 15,063 protein-coding genes in total. As FPKM normalisation does not effectively
707 account for cross-library variability, we additionally performed two normalisation approaches:

708

709 (a) Quantile normalisation: using all the samples together (n=63, regardless of their age or tissue),
710 FPKM values were log₂ transformed (after adding 1) and quantile normalised with ‘normalize.quantiles’
711 function from ‘preprocessCore’ library v.1.54 (Bolstad 2020). This approach equalises the distributions
712 of different libraries. The assumption is that any large-scale differences in expression level distributions
713 reflect technical factors.

714

715 (b) Variance stabilising transformation (VST): To assess the robustness of quantile normalisation on
716 downstream analysis, we additionally implemented this approach, which ensures homoscedasticity, i.e.
717 variances of expression levels are independent of the mean (Anders and Huber 2010). Uniquely aligned
718 reads obtained from the STAR alignment were used to calculate read counts by HTSeq v.0.13.5
719 (Anders, Pyl, and Huber 2014) with parameters: “--format=bam --order=pos --stranded=no --type=exon
720 --mode=union --nonunique=none”. Read counts were then imported into R using the
721 ‘DESeqDataSetFromHTSeqCount’ function in DESeq2 v.1.32.0 package (Love, Huber, and Anders
722 2014). The same filtration steps were applied as above, resulting in 14,973 protein-coding genes in
723 total. Normalisation was performed with the ‘vst’ function and ‘blinded=T’ option in the DESeq2
724 package. The VST-normalised expression matrix was used to reproduce Figure 1 and Figure 2 results
725 which are given in Figure 1-figure supplement 10, 11 and Figure 2-figure supplement 14.

726

727 Principal component analysis:

728 We studied the main sources of variation in the whole dataset using principal component analysis (PCA)
729 on the scaled expression matrix with 'prcomp' function in the R base. The first four components, PC1
730 to PC4, explained 31%, 20%, 17% and 8% of the total variance. We observed a clear separation of
731 tissues in PC1 and PC2 and a strong age effect in PC4. To statistically confirm tissue differences, we
732 performed ANOVA on individual PC scores with tissue as explanatory variable; this was run on each of
733 the first four PCs (PC1-PC4), separately. The magnitude of the age effect on PCA analysis was
734 measured with Spearman's correlation test between individual age and each individual's PC score,
735 separately in each tissue. PCA was also repeated for development and ageing periods, separately
736 (**Figure 1-figure supplement 3**). We further calculated Euclidean distance in pairwise manner among
737 tissues of each individual in PC1-4 space constructed in three different ways: (a) using all the samples
738 together, (b) using only the developmental samples, (c) using only the ageing samples. Then, we tested
739 the effect of age on mean Euclidean distance among tissues using the Spearman's correlation test. To
740 study only the age effect on PC scores without the tissue effect we performed the following; (i) we
741 removed the tissue-specific effects from the data by scaling the expression levels of each gene to
742 mean=0 and sd=1 in each tissue separately, and (ii) we combined the four scaled expression matrices,
743 (iii) we conducted PCA on the combined dataset (**Figure 1-figure supplement 2**).

744

745 **Age-related gene expression change**

746 To identify genes showing age-related expression change in each tissue, we used Spearman's
747 correlation coefficient between individual age and expression level, separately for development and
748 ageing periods. To capture potential non-linear but monotonic changes in expression, we chose the
749 non-parametric two-sided Spearman's correlation test for both periods. We have used two-sided tests
750 for all statistical tests throughout the article except the permutation tests. Significance of age-related
751 genes was assessed with the **false-discovery-rate** (FDR corrected p-value<0.1 cutoff, calculated with
752 the Benjamini-Hochberg (BH) procedure (Benjamini and Hochberg 1995)) using the 'p.adjust' function
753 in the R base library. Throughout the article, BH procedure with 0.1 cutoff was used for multiple test
754 corrections of all statistical tests.

755

756 Functional associations:

757 We tested the functional associations of age-related gene expression change in separate tissues for
758 each period (development and ageing) separately, employing the gene set over-representation analysis
759 (GORA) procedure with Gene Ontology (GO) (Ashburner et al. 2000) Biological Process (BP)
760 categories using the 'topGO' package v.2.44 (Alexa and Rahnenfuhrer 2019). We applied the 'classical'
761 algorithm and performed Fisher's exact test on categories that satisfy the criteria of a minimum 10 and
762 maximum 500 number of genes. We used the whole set of expressed genes (n=15,063) as the
763 background. P-values were corrected for multiple testing using the BH procedure. Categories with FDR
764 corrected p-value<0.1 were considered as significant.

765

766 **Correlation between age-related gene expression changes in different tissues**

767 We calculated Spearman's correlation coefficients between age-related gene expression change ρ_{gene}
768 values (i.e. correlation between gene expression levels and age) calculated per gene in each tissue
769 pair (**Figure 1c**). In order to test the statistical significance of the correlations, we used a permutation
770 scheme as the expression levels across tissues are not independent but belong to the same mice. In
771 order to account for the dependence, the individual ages were permuted in each round, but the
772 permuted values were kept constant across tissues (similar to permutation tests applied in (Dönertaş
773 et al. 2017; Işıldak et al. 2020; Dönertaş et al. 2018)). Specifically, we performed 1000 permutation
774 rounds. In each round, we randomised the individual ages using the 'sample' function in R, while
775 keeping the permuted age labels constant for individuals across tissues. We calculated the age-related
776 gene expression changes with permuted ages in development and ageing datasets separately, thus
777 simulating the null distribution with no age effect in each period. We then calculated the Spearman's
778 correlation coefficient between the age-related expression levels from the permutations across tissues
779 and assigned the p-value by calculating the proportion of permuted calculations with a more extreme
780 correlation. All permutation tests in the article were performed as one-sided tests. The estimated false-
781 positive-proportion (eFPP; proportion of false positives among all true non-significant results (true
782 negatives+false positives)) was calculated as the median value of expected values divided by the
783 observed value (**Figure 1-source data**).

784

785 **Shared gene expression changes across tissues**

786 We summarised the number of shared age-related genes among tissues for up- and down-regulated
787 genes separately, using FDR corrected p-value<0.1 (**Figure 1-figure supplement 5**). The development
788 and ageing datasets were tested separately. For each gene, we counted the number of tissues with the
789 same direction of expression change with age. We calculated this overlap statistic among tissues (a)
790 using genes with FDR-corrected p-value<0.1, and (b) with all genes without using any significance
791 cutoff (**Figure 1e, Figure 1-figure supplement 4**).

792

793 Permutation test:

794 We again used a permutation scheme to assess the significance of shared age-related genes to
795 account for the dependence among tissues. We tested the significance of shared up- and down-
796 regulated genes, selected with or without an FDR cutoff, in development and in ageing periods
797 separately. We used the age-related expression change values (ρ'_{gene}) calculated by permuting
798 individual ages, 1000 times. To test the significance of the overlap of significantly up- or down- regulated
799 genes (FDR corrected p-value<0.1) among tissues, we used the following procedure: (i) For each
800 permutation round, we ranked the ρ'_{gene} values for each tissue in each period separately. (ii) We chose
801 the highest N_u (to test the up-regulation), or lowest N_d (to test the down-regulation) number of genes,
802 where N_u and N_d are the number of significantly up- or down- regulated genes, respectively, in a given
803 tissue (FDR corrected p-value<0.1). (iii) For each permutation round, we calculated the number of
804 overlaps across tissues using the chosen gene sets, i.e. the number of tissues with the same direction
805 of expression change with age for those genes. Doing this for 1000 permutation results yielded a null
806 distribution representing the expected overlaps if there were no age effect. (iv) We calculated the p-
807 value as the proportion of 1000 permutations where the number of overlaps was higher than the
808 observed value. The estimated false-positive-proportion (eFPP) was calculated as the median number
809 of overlaps in permutations divided by the observed value.

810

811 Likewise, to test the significance of the overlap of shared up- and down-regulated genes selected
812 without FDR cutoff, we used the same permutation scheme explained above, but this time using all the
813 age-related expression changes created using permutations (ρ'_{gene}), without applying a significance
814 cutoff for any tissue, and calculating the overlap across tissues in the same way.

815

816 Functional Associations:

817 We tested the functional associations of shared expression change trends among tissues in each
818 period, separately, following the GORA procedure using the same criteria and algorithms explained in
819 the previous section. To test shared up-regulated (n=45) or down-regulated genes (n=138) in
820 development, we chose all significant age-related genes across tissues (n=10,305) in the development
821 period as background. Since we could not identify any shared ageing-related genes across tissues
822 (**Figure 1-figure supplement 5**), we did not perform a functional test for the ageing period.

823

824 **Analysis of gene expression reversals**

825 We compared the direction of gene expression change during development and during ageing to
826 identify reversal genes in each tissue, separately. Genes showing up-regulation (positive correlation
827 with age) in development and down-regulation (negative correlation with age) in ageing were assigned
828 as up-down (UD) reversal genes, while the genes with the opposite trend (down-regulation in
829 development and up-regulation in ageing) were assigned as down-up (DU) reversal genes. Without
830 using any significance level for expression-age correlation values, we calculated the proportion of genes
831 showing reversal by keeping the expression change direction in development the same, *i.e.*
832 $UD\% = UD / (UU + UD)$ and $DU\% = DU / (DD + DU)$.

833

834 Permutation test:

835 To test the significance of reversal proportions, we kept the developmental changes constant and
836 randomly permuted the individual ages only in the ageing period (as described earlier). Among
837 developmental up-regulated genes, we calculated the UD% in each permutation, simulating a null
838 distribution for UD reversal. We applied the same principle for the DU genes. Thus, we created a null
839 distribution with the expected reversal ratios and tested the significance of observed values for each
840 tissue separately (**Figure 1-figure supplement 8**).

841

842 Functional associations:

843 We used the GORA procedure as described earlier to test functional associations of reversal genes in
844 each tissue but kept the developmental changes constant in the background. More specifically, we

845 tested the functional enrichment of UD reversal genes against UU genes, and DU genes against DD
846 genes. We thereby specifically test the functions associated with the reversal pattern, but not
847 development-associated functions.

848

849 Overlap of reversal genes - permutation test:

850 We tested the significance of overlap using the same permutation scheme described above.
851 Specifically, among developmental up- (or down-) regulated genes shared among tissues, we
852 constructed null distributions by calculating the ratio of UD vs UD+UU (or DU vs DU+DD) genes shared
853 among tissues, identified in 1000 random permutations of individual ages only in the ageing period.
854 **(Figure 1-figure supplement 9)**. The number of shared up-regulated genes was $n_{up}=2,255$ (one gene
855 excluded since it has constant expression in one tissue in ageing period), and the number of shared
856 down-regulated genes was $n_{down}=2,209$.

857

858 **Tissue convergence and divergence calculations using coefficient of variation (CoV)**

859 For each individual mouse, for each gene ($n=15,063$), we calculated the inter-tissue coefficient of
860 variation (CoV) estimate using normalised expression levels from the four tissues, dividing the standard
861 deviation by the mean. We studied inter-tissue expression-variation change with age in development
862 and ageing periods separately, using two approaches: (a) using the change in mean or median CoV
863 across genes, and (b) studying significant CoV patterns at the single gene level.

864

865 Mean/median CoV across all genes:

866 We assessed transcriptome-wide variation among the tissues of each individual mouse by calculating
867 the mean (or median) CoV of genes and then performing the Spearman's correlation test between
868 mean-CoV (or median-CoV) and individual age.

869

870 CoV at the single gene level:

871 In the second approach, we tested the correlation between the CoV value of a gene and individual age
872 for each commonly expressed gene using the Spearman's correlation test. P-values were corrected for
873 multiple testing, using the 'BH' procedure. We used FDR corrected $p\text{-value}<0.1$ as cutoff. The genes
874 showing positive correlation between CoV and age were called "divergent", and the ones showing

875 negative correlation were called “convergent” (**Figure 2b**). Genes that display a divergent pattern during
876 development and convergent pattern in ageing (without using a significance level) were called
877 divergent-convergent (DiCo) genes (n=4,802).

878

879 Permutation Test:

880 To test the significance of DiCo genes (n=4,802), we kept the developmental divergent genes constant
881 (n=9,058, without a significance cutoff) and randomly permuted the individual ages only in the ageing
882 period (as described earlier). Among developmental divergent genes, we calculated the DiCo% for each
883 permutation, simulating a null distribution for the DiCo pattern (**Figure 2-figure supplement 12**).

884

885 Clustering of DiCo genes:

886 We used the k-means algorithm to cluster DiCo genes according to their CoV or expression changes
887 with age, separately (**Figure 2-figure supplement 2-3**). To find the optimum number of clusters for
888 both procedures, we applied gap statistics using the ‘clusGap’ function in the ‘cluster’ package v.2.1.2
889 with 500 simulations (Tibshirani, Walther, and Hastie 2001). We used the ‘kmeans’ function in base R
890 with ‘iter.max=20’ and ‘nstart=50’ parameters to cluster CoV values or expression levels which were
891 standardised to mean=1 and sd=0 across genes.

892

893 Effect of gene expression trajectories on DiCo:

894 To identify potential non-monotonic expression changes with age that could not be detected with the
895 Spearman’s correlation coefficient, we clustered all expressed genes (n=15,063) in each tissue,
896 separately, using the k-means algorithm following the same steps explained above (**Figure 1-figure
897 supplement 12-15**). The list of genes belonging to each cluster is given in **Figure 2-source data**. Then,
898 for each cluster, separately in each tissue, we performed a Fisher’s exact test to assess if a particular
899 cluster pattern is enriched or depleted in DiCo genes relative to all other expressed genes (the
900 background).

901

902 Functional association analysis:

903 To test the functional associations of the genes showing the DiCo pattern among tissues, we performed
904 GSEA using GO BPs. We retrieved developmental divergent genes (with $\rho_{\text{CoV-age}} > 0$, n=9,058) and

905 multiplied these $\rho_{\text{CoV-age}}$ values with the ones calculated in the ageing period. Therefore, the genes with
906 a negative value represent a DiCo pattern, while the ones with a positive value represent a divergent-
907 divergent (DiDi) pattern. We then ranked the genes according to the calculated product values and
908 sought enrichment for the upper and lower tail of the distribution using the Kolmogorov-Smirnov (KS)
909 test implemented in the 'clusterProfiler' package v.4.0.0 (Yu et al. 2012). The 'gseGO' function was
910 used with parameters: "nPerm=1000, minGSSize=10, maxGSSize=500 and pValueCutoff=1".
911 Therefore, the enriched categories for the genes in the lower tail of the distribution would represent
912 DiCo enrichment. Categories with FDR corrected p-value<0.1 were considered as significant.

913

914 We summarised DiCo enriched categories into representative ones following (Dönertaş et al. 2021) and
915 used hierarchical clustering on gene similarities among categories. The tree was cut into 25 clusters.
916 For each cluster, we chose as representative the category that has the highest mean Jaccard similarity
917 to the other categories in the same cluster. Then, we calculated the mean age-expression correlation
918 across all the genes in each representative category, in each tissue and in each period. As the unrelated
919 categories, those with the low within cluster similarity, were grouped into one cluster, we denoted them
920 'Other GO', and performed the same clustering steps to further summarise them (**Figure 4-figure**
921 **supplement 1**).

922

923 We further sought functional enrichment among DiCo genes that were clustered with the k-means
924 algorithm for both CoV and expression clusters, separately (**Figure 2-figure supplement 2-3**). Genes
925 in each cluster were tested among all DiCo genes using the same GORA procedure as described
926 before.

927

928 Jackknife to test the Di/Co ratio between dev and ageing:

929 We tested the significance of divergent/convergent gene ratios using a jackknife resampling procedure
930 in development and in ageing periods, separately. Leaving out an individual in each iteration, we re-
931 calculated the number of significant divergent and convergent genes and their ratios. As we could not
932 obtain any gene with significant CoV changes when the youngest adults were left-out due to the
933 decreased power, standard error and confidence interval calculation was not possible. Instead, we
934 report the range of pseudovalues. We note that the range of ratios in leave-out samples do not contain

935 the value 1 either in the development (0.41-0.49) or in the ageing (1.20-2.83) period (**Figure 2e**).

936

937 **Pairwise tissue divergence-convergence test**

938 In order to further verify the inter-tissue divergent-convergent pattern that we observed between
939 development and ageing periods, we used a different approach based on expression correlations
940 among tissues. We calculated pairwise Spearman's correlation coefficients among tissues of the same
941 individual mouse, using all commonly expressed genes among the tissues (n=15,063). For each tissue
942 pair, we tested the correlation between age and inter-tissue expression-correlations using the
943 Spearman's correlation test in development and in ageing periods, separately. In addition, we calculated
944 the mean (or median) of all six pairwise tissue correlations for each individual mouse, and tested the
945 correlation between age and average inter-tissue expression-correlations using the Spearman's
946 correlation test (**Figure 2-figure supplement 6**).

947

948 **Determination of tissue-specific genes**

949 To identify which tissue(s) contribute to the reversal pattern, we assigned each gene to a tissue to
950 identify tissue-specific expression patterns. First, we calculated an effect size (ES) between the
951 expression of a gene in a tissue versus other three tissues using the development samples only, and
952 repeated this procedure for all tissues. Hence, we obtained ES for each commonly expressed gene in
953 each tissue. ES was calculated using the 'Cohen's d' formula defined as the difference between the two
954 means divided by the pooled standard deviation. We then assigned each gene to a tissue in which the
955 gene has the highest ES. Finally, we retrieved only the fourth quartile (>Q3) of genes assigned to a
956 tissue to define tissue-specific expression. Using this approach, we identified 3,766 tissue-specific
957 genes in total (cortex: 1,175, lung: 839, liver: 986, muscle: 766 genes).

958

959 Enrichment test with the direction of age-related change:

960 We tested the association between tissue-specificity and age-related expression change during ageing
961 using Fisher's exact test. Specifically, we constructed a contingency table with two categorical variables;
962 the first variable defines the direction (either positive or negative) of maximum expression change during
963 ageing identified in a tissue-specific gene, which is determined by the slope of the regression between
964 log₂ age and expression. The second variable defines whether this maximum expression change

965 identified in a tissue-specific gene occurs in its native tissue or not (either yes or no). Hence, a positive
966 odds ratio (OR) suggests that (a) either the expression of genes decrease the most in their native tissue,
967 and/or (b) the expression of genes increase the most in a non-native tissue during ageing.

968

969 *Enrichment of tissue-specific genes in DiCo genes:*

970 We tested the association between tissue-specificity [being either tissue-specific (n=3,766) or not
971 (n=11,297)] and the DiCo pattern [either showing DiCo (n=4,802) or not (n=10,261)] using the Fisher's
972 exact test, calculating the enrichment of tissue-specific genes within DiCo genes.

973

974 **Additional publicly available bulk tissue transcriptome datasets**

975 *Jonker:*

976 We downloaded the raw data from the GEO database with GSE34378 accession number (Jonker et al.
977 2013) and followed the same analysis pipeline described above using all the samples from 5 tissues
978 ("Brain - Cortex", "Lung", "Liver", "Kidney", "Spleen") of 18 female mice comprising 90 samples in total.
979 This dataset represents the ageing period of the mouse, ranging from 90 to 900 days. Using the oligo
980 package v.1.56.0 (Carvalho and Irizarry 2010), we retrieved the expression matrices and performed
981 "rma" normalisation followed by removing the probesets that were annotated to more than one gene.
982 We confined the analysis to only the protein-coding genes expressed in at least 25% of all samples.
983 The resulting 17,661 genes were log2 transformed (after adding 1) and quantile normalised using the
984 preprocessCore library (Bolstad 2020) across all samples. Downstream analysis was the same as
985 described above.

986

987 *Schaum:*

988 We downloaded the raw count matrix from the GEO database with GSE132040 accession number
989 (Schaum et al. 2020) and performed the same filtering steps as described above. We discarded the
990 samples that have less than 4 million reads which was the cutoff used in the article. We restricted the
991 analysis to only protein-coding genes expressed in at least 25% of the samples that have expression
992 in 4 tissues ("Brain", "Lung", "Liver", "Muscle"). One individual was removed from the analysis due to
993 being an outlier in PCA analysis after visual inspection (mouse ID: '3m7', PCA plots before and after
994 outlier removal are present in our github repository). Final dataset contained 16,806 protein-coding

995 genes from 37 mice that range from 3 to 27 months of age covering the ageing period. There were 11
996 female mice ranging from 3 to 21 months of age and 26 male mice ranging from 3 to 27 months of age.
997 We performed the same normalisation method and downstream analyses described above. We
998 extended the analysis to 8 tissues ("Brain", "Heart", "Kidney", "Liver", "Lung", "Muscle", "Spleen",
999 "Subcutaneous Fat") which were chosen based on the highest number of individuals that have the same
1000 tissue samples and that cover the whole ageing period (3 to 27 months). For the fat tissue,
1001 "Subcutaneous Fat" was chosen as representative tissue which has the highest number of samples
1002 among all minor fat tissues. After performing the same preprocessing steps explained above, the final
1003 dataset contained 17,619 genes from 26 mice. Downstream analysis was the same as above.

1004

1005 GTEX:

1006 We downloaded the processed GTEx v8 dataset (GTEx Consortium et al. 2017) from the data portal
1007 and repeated the analysis in human tissues. We first confirmed our results in the same 4 tissues ("Brain
1008 - Cortex", "Lung", "Liver", "Muscle - Skeletal") and then expanded the analysis to 10 tissues ("Adipose
1009 - Subcutaneous", "Artery - Tibial", "Brain - Cerebellum", "Lung", "Muscle - Skeletal", "Nerve - Tibial",
1010 "Pituitary", "Skin - Sun Exposed (Lower leg)", "Thyroid", "Whole Blood"). In order to choose which
1011 tissues to analyse, we first choose the minor tissues with the highest number of samples for each major
1012 tissue, which prevents the representation of the same tissue multiple times. We then performed
1013 hierarchical clustering of tissues based on the presence of samples from the same individuals (**Figure**
1014 **2-figure supplement 13**) and cut the tree into 3 clusters based on visual inspection. We selected the
1015 cluster with the highest number of overlapping individuals to analyse. The same procedure was followed
1016 for both 4- and 10-tissue analyses. In particular, we restricted the analysis to the individuals with
1017 samples in all tissues analysed and with a death circumstance of 1 (violent and fast deaths due to an
1018 accident) and 2 (fast death of natural causes) on the Hardy Scale (n =47 for 4 tissue, n=35 for 10 tissue).
1019 We removed duplicated genes from the analysis. Similar to our analysis with the mice data, we used
1020 only the protein-coding genes that are expressed in at least 25% of all samples, totalling 16,197 for 4
1021 tissues and 16,305 for 10 tissues. The TPM values obtained from the GTEx data portal were log2
1022 transformed (after adding 1), and quantile normalised using the preprocessCore library (Bolstad 2020)
1023 in R. Downstream analysis was the same as other datasets. To study the sex-specific convergence
1024 patterns, we repeated the same analysis separating female (n=11) and male (n=36) individuals.

1025 **Table 2.** Dataset characteristics summarising species, tissues, number of individuals, age range, sex,
1026 and platform used for measuring gene expression values.

Dataset	Species	Tissues	N	Age range	Sex	Method
Izgi et al. 4 tissues	Mice	Brain, lung, liver, muscle	8	3 to 30 months	Male	RNAseq
Jonker et al. 5 tissues	Mice	Brain, lung, liver, kidney, spleen	18	3 to 30 months	Female	Microarray
Schaum et al. 4 tissues	Mice	Brain, lung, liver, muscle	37	3 to 27 months	Male (n=26) Female (n=11)	RNAseq
Schaum et al. 8 tissues	Mice	Brain, lung, liver, muscle, subcutaneous fat, kidney, heart, spleen	26	3 to 27 months	Male (n=20) Female (n=6)	RNAseq
GTEx 4 tissues	Humans	Brain, lung, liver, muscle	47	20 to 75 years	Male (n=36) Female (n=11)	RNAseq
GTEx 10 tissues	Humans	Adipose, tibial artery, cerebellum, lung, skeletal muscle, tibial nerve, pituitary, sun-exposed skin, thyroid, and whole blood	35	20 to 75 years	Male (n=27) Female (n=8)	RNAseq

1027

1028

1029 **Comparison of datasets**

1030 We compared the age-related expression change patterns across tissues of all datasets analysed using
1031 Spearman's correlation coefficient. We used the 'pheatmap' function from pheatmap package v1.0.12
1032 (Raivo 2019) using hierarchical clustering (**Figure 4-figure supplement 2a**).

1033

1034 We performed Fisher's exact test to test the enrichment of convergent genes among datasets during
1035 ageing. We used only the convergent genes in ageing in our dataset (n=7,748) for comparison. For
1036 GTEx and Schaum et al. datasets, we performed enrichment for the same four tissues as our dataset
1037 and also for the larger sets, indicated as GTEx10 and Schaum8, respectively (**Figure 4-figure
1038 supplement 2b**).

1039

1040 **Regulatory analysis**

1041 We used MiRTarBase (downloaded in 03/08/2021) (Hsu et al. 2010, 2014) and TRANSFAC
1042 (downloaded in 03/08/2021) (Matys et al. 2003, 2006) resources from the Ma'ayan lab database
1043 (Rouillard et al. 2016) for miRNA and transcription factor binding site (TFBS) enrichment analyses,
1044 respectively. As the database contains target information only for human HGNC IDs, we first converted

1045 those IDs to human Ensembl IDs and then to mouse Ensembl IDs only for the one-to-one ortholog
1046 genes, using 'getBM' and 'getLDS' functions from the biomaRt package. In total, we analysed 235
1047 miRNAs associated with 5,458 target genes and 158 TFs associated with 7,427 target genes. We
1048 conducted the overrepresentation analysis in the same way as for the DiCo functional enrichment
1049 analysis: specifically, we tested the targets of each regulator for enrichment in -Co genes (convergent
1050 genes in ageing) among Di- genes (divergent genes in development) used as background to keep
1051 developmental patterns fixed. We restricted the analysis for miRNA and TFs that have at least 5 target
1052 genes. After multiple testing correction with the BH procedure, we found no enrichment among either
1053 of the regulator types. Enrichment results are given in **Figure 4-source data**.

1054

1055 **Heteroscedasticity tests on the DiCo pattern**

1056 To test the hypothesis that the convergence pattern observed in the ageing period could be explained
1057 by the increased noise with age, thus regression towards the mean, we performed two distinct
1058 heteroscedasticity tests to compare DiCo genes against the lifelong-divergent genes (DiDi). In the first,
1059 we followed the method used to measure heteroscedasticity in Isildak et al. (2020) and Kedlian et al.
1060 (2019). We first fit a linear model between log2 transformed age and expression level, for each gene in
1061 each tissue (Kedlian et al. 2019; Işıldak et al. 2020; Somel et al. 2006). This represents the variability
1062 of error along the explanatory variable, age. Then, we calculated Spearman's correlation coefficient
1063 between the absolute residual values and age, which can be used as an estimate of heterogeneity
1064 change with age. We compared the heterogeneity change values of DiCo and DiDi genes using a two-
1065 sided KS test in each tissue. In the second approach, we used the 'ncvTest' function from the 'car'
1066 package v.3.0.11 (Fox and Weisberg 2018) which is a chi-squared test for heteroscedasticity estimated
1067 using a linear model. Again, we compared the heteroscedasticity measures of DiCo and DiDi genes
1068 using a two-sided KS test in each tissue.

1069

1070 **Single-cell RNAseq**

1071 Preprocessing:

1072 We used the Tabula Muris Senis dataset (Tabula Muris Consortium 2020) for scRNA-seq analysis as
1073 it is the only dataset to our knowledge that includes time-series samples covering old age, and the
1074 tissues present in our dataset. Seurat-processed FACS data of the tissues lung, liver, skeletal muscle

1075 and non-myeloid brain were downloaded from the figshare database (Pisco 2020). The Seurat package
1076 v.4.0.0 (Stuart et al. 2019) was used to retrieve the expression matrix of the cells that are annotated to
1077 cell types in the original article. Each tissue contains samples from three time points: 90 (3m), 540 (18m)
1078 and 720 (24m) days-old mice, totalling 14 samples each in lung, liver and brain, and 9 samples in liver.
1079 We excluded cell types with less than 15 cells among all samples, and excluded genes if the expression
1080 level is 0 for all cells at a given age. This resulted in a median number of 99-382 cells assigned to cell
1081 types, 6-24 cell types and 16,951-22,122 genes across tissues. Using 3-month-old mice, we calculated
1082 cell type-specific expressions in each tissue. Specifically, we first calculated the mean expression levels
1083 among cells of an individual mouse for each cell type, and then calculated the mean among individuals
1084 to obtain an average expression value for each cell type. Uniprot gene symbols were converted to
1085 Ensembl gene IDs using the “biomaRt” R package (Durinck et al. 2009).

1086

1087 Deconvolution:

1088 We used cell type-specific expression profiles of 3-month-old mice to estimate relative contributions of
1089 cell types to the transcriptome profiles of tissues in our mouse dataset. For a given tissue in our mouse
1090 dataset, we used single cell expression profiles of that tissue from the Tabula Muris Senis dataset. We
1091 used a linear regression-based deconvolution method for each tissue using three genesets: all genes
1092 (n=[12,492, 12,849]), DiCo genes (n=[4,007, 4,106]) and non-DiCo genes (n=[8,485, 8,743]).
1093 Regression coefficients were used as relative contributions of cell types according to the following linear
1094 model:

1095

$$1096 Y_i = a + b_{j1} * X_{i1} + b_{j2} * X_{i2} + \dots + b_{jn} * X_{in},$$

1097 where i represents the tissue,

1098 Y_i is the expression level of a sample in a tissue,

1099 $b_{j1...jn}$ represent the relative contributions of the n cell types in a tissue,

1100 $X_{i1...in}$ represent the expression levels of the n cell types in a tissue.

1101

1102 We then tested the effect of age on cell type contributions (b_{j1}, \dots, b_{jn}) using the Spearman's correlation
1103 test in development and in ageing.

1104

1105 Cell type similarities and their change during ageing:

1106 To investigate the contribution of cell autonomous changes to inter-tissue convergence in ageing, we
1107 calculated pairwise cell type expression correlations among tissues and studied how these correlations
1108 change with age. Based on pairwise correlations in the 3-months age group, we identified the maximally
1109 and minimally correlated cell type pairs among tissues. Specifically, for each cell type in a given tissue,
1110 we chose the minimally correlated cell type in each of the other three tissues. For example, for each of
1111 the 10 cell types in the liver, we chose the minimally correlated cell type among the 15 cortex cell types,
1112 the minimally correlated cell type among the 24 lung cell types, and the minimally correlated cell type
1113 among the 6 muscle cell types. We repeated this procedure for all cell types in all four tissues, resulting
1114 in 54 cell type pairs. Then, we calculated Spearman's correlation coefficients between age and
1115 minimally correlated cell type pairs identified in the 3-months age group. Likewise, we repeated the
1116 same analysis for the maximally correlated cell type pairs among tissues.

1117

1118 Permutation tests:

1119 To test whether DiCo genes are significantly more associated with cell type proportion changes than
1120 non-DiCo genes, we performed a permutation test based on a re-sampling procedure. For each tissue,
1121 we took random samples among all genes ($n=[12,492, 12,849]$) with size N , where N is the number of
1122 DiCo genes in that tissue, and repeated the deconvolution analysis as explained above. By calculating
1123 cell type proportion changes with age for each random sample repeated 1000 times, we created the
1124 null distribution for each cell type. Then, we calculated the p-values as the number of random samples
1125 having the same or higher cell type proportion change values divided by the observed value (cell type
1126 proportion changes with DiCo genes).

1127

1128 We applied a similar permutation scheme as explained above to test cell type similarity change
1129 differences between DiCo and non-DiCo genes. For each random sample of non-DiCo genes with size
1130 N , we calculated the pairwise correlations among cell types of tissues and identified maximally and
1131 minimally correlated cell types in the 3-months age group. Then, we calculated age-related changes of
1132 those correlations using Spearman's correlation coefficient to construct the null distribution.

1133

1134 *Analysis of within-tissue convergence of cell types:*

1135 Analogous to inter-tissue convergence analysis, we also studied intra-tissue convergence of cell types
1136 in scRNA-seq data by calculating CoV among cell types within a tissue for each individual of ages 3m,
1137 18m and 24m, separately. We filtered the data to obtain cell types present in at least 2 individual mice
1138 in every time point for each tissue which yielded 4, 7, 20 and 6 cell types in brain, liver, lung and muscle,
1139 respectively. We then tested the mean CoV (or CoV per gene) change with age using Spearman's
1140 correlation test.

1141

1142 **Ethics statement**

1143 Post-mortem samples were obtained from 16 C57BL/6J mice aged between 2 days and 904 days. All
1144 mouse experiments were overseen by the Institutional Animal Welfare Officer of the Max Planck
1145 Institute for Evolutionary Anthropology (MPI-EVA). They were performed according to the German
1146 Animal Welfare Legislation, ("Tierschutzgesetz") and registered with the Federal State Authority
1147 Landesdirektion Sachsen (No. 24-9162. 11-01 (T62/08)). The mice were sacrificed for reasons
1148 independent of this study, their tissues were harvested and frozen immediately, and stored at -80°C.

1149

1150 **Competing Interests**

1151 The authors report no competing interests.

1152

1153 **Data Availability**

1154 Raw and processed RNA-seq data have been deposited in GEO with the accession number
1155 GSE167665. All summary statistics and analysis output are also provided as supplementary tables.

1156

1157 **Code Availability**

1158 All the code used to perform analyses is available in GitHub: https://github.com/hmtzg/geneexp_mouse

1159

1160 **Author Contributions**

1161 H.I., H.M.D, M.S. and P.K. conceived and conceptualised the study. H.I, H.M.D, and M.S. design the
1162 models to analyse the data. U.I. and H.M.D validated the results. H.I. analysed the data with

1163 contributions by U.I., H.M.D, and E.K. D.D.H conducted the experiments and produced the raw data.
1164 S.H. helped D.D.H. with experimental procedures. H.I., U.I., H.M.D. curated and visualised the data.
1165 H.I., H.M.D., and M.S. wrote the manuscript. M.S and P.K. acquired funding for the experiments.
1166 H.M.D., M.S., and P.K. supervised and administered the study. All authors read, revised and approved
1167 the final version of this manuscript.

1168

1169 **Acknowledgement**

1170 We thank Wolfgang Enard and Wulf Hevers for help with the mouse experiments and sharing samples,
1171 Nurcan Tuncbag, Nihal Terzi Çizmecioğlu, and the whole METU CompEvo team for helpful comments
1172 and fruitful discussions, and Zeliha Gözde Turan and Melih Yıldız for the critical reading of the
1173 manuscript and their suggestions.

1174

1175 **Funding Statement**

1176 This work was supported by EMBL (H.M.D), the Scientific and Technological Research Council of
1177 Turkey (TÜBİTAK 2232, M.S.), the Science Academy (of Turkey) BAGEP Award (M.S.), and a METU
1178 Internal Grant (BAP, M.S.).

1179

1180 **References**

- 1181 Alexa, Adrian, and Jorg Rahnenfuhrer. 2019. "topGO: Enrichment Analysis for Gene Ontology."
1182 Anders, Simon, and Wolfgang Huber. 2010. "Differential Expression Analysis for Sequence Count
1183 Data." *Genome Biology* 11 (10): R106.
1184 Anders, Simon, Paul Theodor Pyl, and Wolfgang Huber. 2014. "HTSeq—a Python Framework to
1185 Work with High-Throughput Sequencing Data." *Bioinformatics* 31 (2): 166–69.
1186 Andrews, Simon. 2010. "FastQC: A Quality Control Tool for High Throughput Sequence Data." 2010.
1187 <http://www.bioinformatics.babraham.ac.uk/projects/fastqc/>.
1188 Angelidis, Ilias, Lukas M. Simon, Isis E. Fernandez, Maximilian Strunz, Christoph H. Mayr, Flavia R.
1189 Greiffo, George Tsitsiridis, et al. 2019. "An Atlas of the Aging Lung Mapped by Single Cell
1190 Transcriptomics and Deep Tissue Proteomics." *Nature Communications* 10 (1): 963.
1191 Anisimova, Aleksandra S., Mark B. Meerson, Maxim V. Gerashchenko, Ivan V. Kulakovskiy, Sergey

- 1192 E. Dmitriev, and Vadim N. Gladyshev. 2020. “Multifaceted Deregulation of Gene Expression and
1193 Protein Synthesis with Age.” *Proceedings of the National Academy of Sciences of the United*
1194 *States of America*, June. <https://doi.org/10.1073/pnas.2001788117>.
- 1195 Ashburner, M., C. A. Ball, J. A. Blake, D. Botstein, H. Butler, J. M. Cherry, A. P. Davis, et al. 2000.
1196 “Gene Ontology: Tool for the Unification of Biology. The Gene Ontology Consortium.” *Nature*
1197 *Genetics* 25 (1): 25–29.
- 1198 Bahar, Rumana, Claudia H. Hartmann, Karl A. Rodriguez, Ashley D. Denny, Rita A. Busuttill, Martijn
1199 E. T. Dollé, R. Brent Calder, et al. 2006. “Increased Cell-to-Cell Variation in Gene Expression in
1200 Ageing Mouse Heart.” *Nature* 441 (7096): 1011–14.
- 1201 Benjamini, Yoav, and Yosef Hochberg. 1995. “Controlling the False Discovery Rate: A Practical and
1202 Powerful Approach to Multiple Testing.” *Journal of the Royal Statistical Society. Series B,*
1203 *Statistical Methodology* 57 (1): 289–300.
- 1204 Blagosklonny, Mikhail V. 2006. “Aging and Immortality: Quasi-Programmed Senescence and Its
1205 Pharmacologic Inhibition.” *Cell Cycle* 5 (18): 2087–2102.
- 1206 Bolger, Anthony M., Marc Lohse, and Bjoern Usadel. 2014. “Trimmomatic: A Flexible Trimmer for
1207 Illumina Sequence Data.” *Bioinformatics* 30 (15): 2114–20.
- 1208 Bolstad, Ben. 2020. “preprocessCore: A Collection of Pre-Processing Functions.”
1209 <https://github.com/bmbolstad/preprocessCore>.
- 1210 Brawand, David, Magali Soumillon, Anamaria Necsulea, Philippe Julien, Gábor Csárdi, Patrick
1211 Harrigan, Manuela Weier, et al. 2011. “The Evolution of Gene Expression Levels in Mammalian
1212 Organs.” *Nature* 478 (7369): 343–48.
- 1213 Cardoso-Moreira, Margarida, Jean Halbert, Delphine Valloton, Britta Velten, Chunyan Chen, Yi Shao,
1214 Angélica Liechti, et al. 2019. “Gene Expression across Mammalian Organ Development.” *Nature*
1215 571 (7766): 505–9.
- 1216 Carvalho, Benilton S., and Rafael A. Irizarry. 2010. “A Framework for Oligonucleotide Microarray
1217 Preprocessing.” *Bioinformatics* 26 (19): 2363–67.
- 1218 Colantuoni, Carlo, Barbara K. Lipska, Tianzhang Ye, Thomas M. Hyde, Ran Tao, Jeffrey T. Leek,
1219 Elizabeth A. Colantuoni, et al. 2011. “Temporal Dynamics and Genetic Control of Transcription in
1220 the Human Prefrontal Cortex.” *Nature* 478 (7370): 519–23.
- 1221 Dobin, Alexander, Carrie A. Davis, Felix Schlesinger, Jorg Drenkow, Chris Zaleski, Sonali Jha,

- 1222 Philippe Batut, Mark Chaisson, and Thomas R. Gingeras. 2013. "STAR: Ultrafast Universal RNA-
1223 Seq Aligner." *Bioinformatics* 29 (1): 15–21.
- 1224 Dönertaş, Handan Melike, Daniel K. Fabian, Matías Fuentealba Valenzuela, Linda Partridge, and
1225 Janet M. Thornton. 2021. "Common Genetic Associations between Age-Related Diseases."
1226 *Nature Aging* 1 (4): 400–412.
- 1227 Dönertaş, Handan Melike, Matías Fuentealba Valenzuela, Linda Partridge, and Janet M. Thornton.
1228 2018. "Gene Expression-Based Drug Repurposing to Target Aging." *Aging Cell* 17 (5): e12819.
- 1229 Dönertaş, Handan Melike, Hamit İzgi, Altuğ Kamacıoğlu, Zhisong He, Philipp Khaitovich, and Mehmet
1230 Somel. 2017. "Gene Expression Reversal toward Pre-Adult Levels in the Aging Human Brain and
1231 Age-Related Loss of Cellular Identity." *Scientific Reports* 7 (1): 5894.
- 1232 Durinck, Steffen, Paul T. Spellman, Ewan Birney, and Wolfgang Huber. 2009. "Mapping Identifiers for
1233 the Integration of Genomic Datasets with the R/Bioconductor Package biomaRt." *Nature*
1234 *Protocols* 4 (8): 1184–91.
- 1235 Enge, Martin, H. Efsun Arda, Marco Mignardi, John Beausang, Rita Bottino, Seung K. Kim, and
1236 Stephen R. Quake. 2017. "Single-Cell Analysis of Human Pancreas Reveals Transcriptional
1237 Signatures of Aging and Somatic Mutation Patterns." *Cell* 171 (2): 321–30.e14.
- 1238 Ezcurra, Marina, Alexandre Benedetto, Thanet Sornda, Ann F. Gilliat, Catherine Au, Qifeng Zhang,
1239 Sophie van Schelt, et al. 2018. "C. Elegans Eats Its Own Intestine to Make Yolk Leading to
1240 Multiple Senescent Pathologies." *Current Biology: CB* 28 (20): 3352.
- 1241 Feser, Jason, David Truong, Chandrima Das, Joshua J. Carson, Jeffrey Kieft, Troy Harkness, and
1242 Jessica K. Tyler. 2010. "Elevated Histone Expression Promotes Life Span Extension." *Molecular*
1243 *Cell* 39 (5): 724–35.
- 1244 Fisher, R. A. (1930). *The genetical theory of natural selection*. 272.
1245 <https://doi.org/10.5962/bhl.title.27468>
- 1246 Flurkey, Kevin, Joanne M. Curren, and D. E. Harrison. 2007. "Chapter 20 - Mouse Models in Aging
1247 Research." In *The Mouse in Biomedical Research (Second Edition)*, edited by James G. Fox,
1248 Muriel T. Davisson, Fred W. Quimby, Stephen W. Barthold, Christian E. Newcomer, and Abigail
1249 L. Smith, 637–72. Burlington: Academic Press.
- 1250 Fox, John, and Sanford Weisberg. 2018. *An R Companion to Applied Regression*. SAGE
1251 Publications.

- 1252 Gems, David, and Linda Partridge. 2013. "Genetics of Longevity in Model Organisms: Debates and
1253 Paradigm Shifts." *Annual Review of Physiology* 75: 621–44.
- 1254 GTEx Consortium, Laboratory, Data Analysis & Coordinating Center (LDACC)—Analysis Working
1255 Group, Statistical Methods groups—Analysis Working Group, Enhancing GTEx (eGTEx) groups,
1256 NIH Common Fund, NIH/NCI, NIH/NHGRI, et al. 2017. "Genetic Effects on Gene Expression
1257 across Human Tissues." *Nature* 550 (7675): 204–13.
- 1258 Hernando-Herraez, Irene, Brendan Evano, Thomas Stubbs, Pierre-Henri Commere, Marc Jan
1259 Bonder, Stephen Clark, Simon Andrews, Shahragim Tajbakhsh, and Wolf Reik. 2019. "Ageing
1260 Affects DNA Methylation Drift and Transcriptional Cell-to-Cell Variability in Mouse Muscle Stem
1261 Cells." *Nature Communications* 10 (1): 4361.
- 1262 Hsu, Sheng-Da, Feng-Mao Lin, Wei-Yun Wu, Chao Liang, Wei-Chih Huang, Wen-Ling Chan, Wen-
1263 Ting Tsai, et al. 2010. "miRTarBase: A Database Curates Experimentally Validated microRNA–
1264 target Interactions." *Nucleic Acids Research* 39 (suppl_1): D163–69.
- 1265 Hsu, Sheng-Da, Yu-Ting Tseng, Sirjana Shrestha, Yu-Ling Lin, Anas Khaleel, Chih-Hung Chou,
1266 Chao-Fang Chu, et al. 2014. "miRTarBase Update 2014: An Information Resource for
1267 Experimentally Validated miRNA-Target Interactions." *Nucleic Acids Research* 42 (Database
1268 issue): D78–85.
- 1269 Işıldak, Ulaş, Mehmet Somel, Janet M. Thornton, and Handan Melike Dönertaş. 2020. "Temporal
1270 Changes in the Gene Expression Heterogeneity during Brain Development and Aging." *Scientific
1271 Reports* 10 (1): 4080.
- 1272 Jonker, Martijs J., Joost Pm Melis, Raoul V. Kuiper, Tessa V. van der Hoeven, P. F. K. Wackers, Joke
1273 Robinson, Gijsbertus Tj van der Horst, et al. 2013. "Life Spanning Murine Gene Expression
1274 Profiles in Relation to Chronological and Pathological Aging in Multiple Organs." *Aging Cell* 12
1275 (5): 901–9.
- 1276 Kedlian, Veronika R., Handan Melike Donertas, and Janet M. Thornton. 2019. "The Widespread
1277 Increase in Inter-Individual Variability of Gene Expression in the Human Brain with Age." *Aging
1278* 11 (8): 2253–80.
- 1279 Kim, S., B. Villeponteau, and S. M. Jazwinski. 1996. "Effect of Replicative Age on Transcriptional
1280 Silencing near Telomeres in *Saccharomyces Cerevisiae*." *Biochemical and Biophysical Research
1281 Communications* 219 (2): 370–76.

- 1282 Lind, Martin I., Sanjana Ravindran, Zuzana Sekajova, Hanne Carlsson, Andrea Hinas, and Alexei A.
1283 Maklakov. 2019. "Experimentally Reduced insulin/IGF-1 Signaling in Adulthood Extends Lifespan
1284 of Parents and Improves Darwinian Fitness of Their Offspring." *Evolution Letters* 3 (2): 207–16.
- 1285 Liu, Xiling, Dingding Han, Mehmet Somel, Xi Jiang, Haiyang Hu, Patricia Guijarro, Ning Zhang, et al.
1286 2016. "Disruption of an Evolutionarily Novel Synaptic Expression Pattern in Autism." *PLoS*
1287 *Biology* 14 (9): e1002558.
- 1288 Love, Michael I., Wolfgang Huber, and Simon Anders. 2014. "Moderated Estimation of Fold Change
1289 and Dispersion for RNA-Seq Data with DESeq2." *Genome Biology* 15 (12): 550.
- 1290 Luegmayr, E., H. Glantschnig, G. A. Wesolowski, M. A. Gentile, J. E. Fisher, G. A. Rodan, and A. A.
1291 Reszka. 2004. "Osteoclast Formation, Survival and Morphology Are Highly Dependent on
1292 Exogenous Cholesterol/lipoproteins." *Cell Death and Differentiation* 11 Suppl 1 (July): S108–18.
- 1293 Magalhães, João Pedro de, and George M. Church. 2005. "Genomes Optimize Reproduction: Aging
1294 as a Consequence of the Developmental Program." *Physiology* 20 (August): 252–59.
- 1295 Martinez-Jimenez, Celia Pilar, Nils Eling, Hung-Chang Chen, Catalina A. Vallejos, Aleksandra A.
1296 Kolodziejczyk, Frances Connor, Lovorka Stojic, et al. 2017. "Aging Increases Cell-to-Cell
1297 Transcriptional Variability upon Immune Stimulation." *Science* 355 (6332): 1433–36.
- 1298 Matys, V., E. Fricke, R. Geffers, E. Gößling, M. Haubrock, R. Hehl, K. Hornischer, et al. 2003.
1299 "TRANSFAC® : Transcriptional Regulation, from Patterns to Profiles." *Nucleic Acids Research*
1300 31 (1): 374–78.
- 1301 Matys, V., O. V. Kel-Margoulis, E. Fricke, I. Liebich, S. Land, A. Barre-Dirrie, I. Reuter, et al. 2006.
1302 "TRANSFAC® and Its Module TRANSCompel®: Transcriptional Gene Regulation in
1303 Eukaryotes." *Nucleic Acids Research* 34 (suppl_1): D108–10.
- 1304 Medawar, P. B. (1953). Unsolved problem of biology. *The Medical Journal of Australia*, 1(24), 854–
1305 855.
- 1306 Pisco, Angela. 2020. "Tabula Muris Senis Data Objects."
1307 <https://doi.org/10.6084/m9.figshare.12654728.v1>.
- 1308 Raivo, Kolde. 2019. "Pheatmap: Pretty Heatmaps." *R Package Version* 1 (8).
- 1309 Rouillard, Andrew D., Gregory W. Gundersen, Nicolas F. Fernandez, Zichen Wang, Caroline D.
1310 Monteiro, Michael G. McDermott, and Avi Ma'ayan. 2016. "The Harmonizome: A Collection of
1311 Processed Datasets Gathered to Serve and Mine Knowledge about Genes and Proteins."

- 1312 *Database: The Journal of Biological Databases and Curation* 2016 (July).
- 1313 <https://doi.org/10.1093/database/baw100>.
- 1314 Sampathkumar, Nirmal K., Juan I. Bravo, Yilin Chen, Prakroothi S. Danthi, Erin K. Donahue, Rochelle
1315 W. Lai, Ryan Lu, Lewis T. Randall, Nika Vinson, and Bérénice A. Benayoun. 2020. "Widespread
1316 Sex Dimorphism in Aging and Age-Related Diseases." *Human Genetics* 139 (3): 333–56.
- 1317 Schaum, Nicholas, Benoit Lehallier, Oliver Hahn, Róbert Pálovics, Shayan Hosseinzadeh, Song E.
1318 Lee, Rene Sit, et al. 2020. "Ageing Hallmarks Exhibit Organ-Specific Temporal Signatures."
1319 *Nature* 583 (7817): 596–602.
- 1320 Somel, Mehmet, Song Guo, Ning Fu, Zheng Yan, Hai Yang Hu, Ying Xu, Yuan Yuan, et al. 2010.
1321 "MicroRNA, mRNA, and Protein Expression Link Development and Aging in Human and
1322 Macaque Brain." *Genome Research* 20 (9): 1207–18.
- 1323 Somel, Mehmet, Philipp Khaitovich, Sabine Bahn, Svante Pääbo, and Michael Lachmann. 2006.
1324 "Gene Expression Becomes Heterogeneous with Age." *Current Biology: CB* 16 (10): R359–60.
- 1325 Stuart, Tim, Andrew Butler, Paul Hoffman, Christoph Hafemeister, Efthymia Papalexi, William M.
1326 Mauck 3rd, Yuhan Hao, Marlon Stoeckius, Peter Smibert, and Rahul Satija. 2019.
1327 "Comprehensive Integration of Single-Cell Data." *Cell* 177 (7): 1888–1902.e21.
- 1328 Tabula Muris Consortium. 2020. "A Single-Cell Transcriptomic Atlas Characterizes Ageing Tissues in
1329 the Mouse." *Nature* 583 (7817): 590–95.
- 1330 Tacutu, Robi, Daniel Thornton, Emily Johnson, Arie Budovsky, Diogo Barardo, Thomas Craig,
1331 Eugene Diana, et al. 2018. "Human Ageing Genomic Resources: New and Updated Databases."
1332 *Nucleic Acids Research* 46 (D1): D1083–90.
- 1333 Tibshirani, Robert, Guenther Walther, and Trevor Hastie. 2001. "Estimating the Number of Clusters in
1334 a Data Set via the Gap Statistic." *Journal of the Royal Statistical Society. Series B, Statistical
1335 Methodology* 63 (2): 411–23.
- 1336 Trapnell, Cole, Brian A. Williams, Geo Pertea, Ali Mortazavi, Gordon Kwan, Marijke J. van Baren,
1337 Steven L. Salzberg, Barbara J. Wold, and Lior Pachter. 2010. "Transcript Assembly and
1338 Quantification by RNA-Seq Reveals Unannotated Transcripts and Isoform Switching during Cell
1339 Differentiation." *Nature Biotechnology* 28 (5): 511–15.
- 1340 Turan, Zeliha Gözde, Poorya Parvizi, Handan Melike Dönertaş, Jenny Tung, Philipp Khaitovich, and
1341 Mehmet Somel. 2019. "Molecular Footprint of Medawar's Mutation Accumulation Process in

- 1342 Mammalian Aging.” *Aging Cell* 348 (May): e12965.
- 1343 Williams, G. C. (1957). Pleiotropy, Natural Selection, and the Evolution of Senescence. *Evolution;*
1344 *International Journal of Organic Evolution*, 11(4), 398–411.
- 1345 Yang, Jae-Hyun, Patrick T. Griffin, Daniel L. Vera, John K. Apostolides, Motoshi Hayano, Margarita V.
1346 Meer, Elias L. Salfati, et al. 2019. “Erosion of the Epigenetic Landscape and Loss of Cellular
1347 Identity as a Cause of Aging in Mammals.” *Cold Spring Harbor Laboratory*.
1348 <https://doi.org/10.1101/808642>.
- 1349 Yang, Jialiang, Tao Huang, Francesca Petralia, Quan Long, Bin Zhang, Carmen Argmann, Yong
1350 Zhao, et al. 2015. “Synchronized Age-Related Gene Expression Changes across Multiple
1351 Tissues in Human and the Link to Complex Diseases.” *Scientific Reports* 5 (October): 15145.
- 1352 Yuan, Yuan, Yi-Ping Phoebe Chen, Jerome Boyd-Kirkup, Philipp Khaitovich, and Mehmet Somel.
1353 2012. “Accelerated Aging-Related Transcriptome Changes in the Female Prefrontal Cortex.”
1354 *Aging Cell* 11 (5): 894–901.
- 1355 Yu, Guangchuang, Li-Gen Wang, Yanyan Han, and Qing-Yu He. 2012. “clusterProfiler: An R Package
1356 for Comparing Biological Themes among Gene Clusters.” *Omics: A Journal of Integrative Biology*
1357 16 (5): 284–87.
- 1358 Zahn, Jacob M., Suresh Poosala, Art B. Owen, Donald K. Ingram, Ana Lustig, Arnell Carter, Ashani T.
1359 Weeraratna, et al. 2007. “AGEMAP: A Gene Expression Database for Aging in Mice.” *PLoS Genetics*
1360 3 (11): e201.